Defense Threat Reduction Agency
8725 John J. Kingman Road, MS
6201 Fort Belvoir, VA 22060-6201

DTRA-TR-16-3

TECHNICAL REPORT

Improved Root Normal Size Distributions for Liquid Atomization

November 2015

HDTRA1-11-D-0004

Culbert B. Laney

Prepared by:
Engility Corp.
8211 Terminal Road
Suite 1000
Lorton, VA 22079

DESTRUCTION NOTICE:

Destroy this report when it is no longer needed.
Do not return to sender.

PLEASE NOTIFY THE DEFENSE THREAT REDUCTION AGENCY, ATTN: DTRIAC/ J9STT, 8725 JOHN J. KINGMAN ROAD, MS-6201, FT BELVOIR, VA 22060-6201, IF YOUR ADDRESS IS INCORRECT, IF YOU WISH IT DELETED FROM THE DISTRIBUTION LIST, OR IF THE ADDRESSEE IS NO LONGER EMPLOYED BY YOUR ORGANIZATION.

REPORT DOCUMENTATION PAGE

Form Approved
OMB No. 0704-0188

1. REPORT DATE *(DD-MM-YYYY)*	**2. REPORT TYPE**	**3. DATES COVERED** *(From - To)*
00-11-2015	Technical	April 18, 2011 - April 17, 2016

4. TITLE AND SUBTITLE

Improved Root Normal Size Distributions for Liquid Atomization

5a. CONTRACT NUMBER

HDTRA1-11-D-0004-0001

5b. GRANT NUMBER

5c. PROGRAM ELEMENT NUMBER

6. AUTHOR(S)

Culbert B. Laney

5d. PROJECT NUMBER

5e. TASK NUMBER

5f. WORK UNIT NUMBER

7. PERFORMING ORGANIZATION NAME(S) AND ADDRESS(ES)

Engility Corp.
8211 Terminal Rd
Suite 1000
Lorton, VA 22079

8. PERFORMING ORGANIZATION REPORT NUMBER

9. SPONSORING / MONITORING AGENCY NAME(S) AND ADDRESS(ES)

Defense Threat Reduction Agency
8725 John J Kingman Rd, STOP 6201
Fort Belvoir, VA 22060

10. SPONSOR/MONITOR'S ACRONYM(S)

DTRA

11. SPONSOR/MONITOR'S REPORT NUMBER(S)

DTRA-TR-16-3

12. DISTRIBUTION / AVAILABILITY STATEMENT

Distribution Statement A. Approved for public release; distribution unlimited.

13. SUPPLEMENTARY NOTES

14. ABSTRACT

This paper identifies two issues with traditional root normal size distributions, of the type used for spray atomization. First, while root normal size distributions are typically expressed in terms of mass mean diameter, they do not actually obtain the correct mass mean diameter. Second, depending on the chosen form, traditional root normal size distributions may exhibit severe non-physical singularities. An alternative root normal size distribution is suggested that avoids these issue. A literature survey finds six possible parameter choices for root normal size distributions. It is found that these parameter choices provide an adequate fit to a wide variety variety of experimental data, except possibly for the largest droplets.

15. SUBJECT TERMS

root normal size distribution, Simmons universal size distribution, spray atomization, probability density function

16. SECURITY CLASSIFICATION OF:			**17. LIMITATION OF ABSTRACT**	**18. NUMBER OF PAGES**	**19a. NAME OF RESPONSIBLE PERSON**
a. REPORT	**b. ABSTRACT**	**c. THIS PAGE**	UU	42	Capt. Paul Clement
Unclassified	Unclassified	Unclassified			**19b. TELEPHONE NUMBER** *(include area code)* 703-767-4035

CONVERSION TABLE

Conversion Factors for U.S. Customary to metric (SI) units of measurement.

MULTIPLY →	BY →	TO GET
TO GET ←	BY ←	DIVIDE
angstrom	1.000 000 x E -10	meters (m)
atmosphere (normal)	1.013 25 x E +2	kilo pascal (kPa)
bar	1.000 000 x E +2	kilo pascal (kPa)
barn	1.000 000 x E -28	meter^2 (m^2)
British thermal unit (thermochemical)	1.054 350 x E +3	joule (J)
calorie (thermochemical)	4.184 000	joule (J)
cal (thermochemical/cm^2)	4.184 000 x E -2	mega joule/m^2 (MJ/m^2)
curie	3.700 000 x E +1	*giga bacquerel (GBq)
degree (angle)	1.745 329 x E -2	radian (rad)
degree Fahrenheit	$t_k = (t^of + 459.67)/1.8$	degree kelvin (K)
electron volt	1.602 19 x E -19	joule (J)
erg	1.000 000 x E -7	joule (J)
erg/second	1.000 000 x E -7	watt (W)
foot	3.048 000 x E -1	meter (m)
foot-pound-force	1.355 818	joule (J)
gallon (U.S. liquid)	3.785 412 x E -3	meter^3 (m^3)
inch	2.540 000 x E -2	meter (m)
jerk	1.000 000 x E +9	joule (J)
joule/kilogram (J/kg) radiation dose absorbed	1.000 000	Gray (Gy)
kilotons	4.183	terajoules
kip (1000 lbf)	4.448 222 x E +3	newton (N)
kip/$inch^2$ (ksi)	6.894 757 x E +3	kilo pascal (kPa)
ktap	1.000 000 x E +2	newton-second/m^2 ($N-s/m^2$)
micron	1.000 000 x E -6	meter (m)
mil	2.540 000 x E -5	meter (m)
mile (international)	1.609 344 x E +3	meter (m)
ounce	2.834 952 x E -2	kilogram (kg)
pound-force (lbs avoirdupois)	4.448 222	newton (N)
pound-force inch	1.129 848 x E -1	newton-meter (N-m)
pound-force/inch	1.751 268 x E +2	newton/meter (N/m)
pound-force/$foot^2$	4.788 026 x E -2	kilo pascal (kPa)
pound-force/$inch^2$ (psi)	6.894 757	kilo pascal (kPa)
pound-mass (lbm avoirdupois)	4.535 924 x E -1	kilogram (kg)
pound-mass-$foot^2$ (moment of inertia)	4.214 011 x E -2	kilogram-meter^2 ($kg-m^2$)
pound-mass/$foot^3$	1.601 846 x E +1	kilogram-meter^3 (kg/m^3)
rad (radiation dose absorbed)	1.000 000 x E -2	**Gray (Gy)
roentgen	2.579 760 x E -4	coulomb/kilogram (C/kg)
shake	1.000 000 x E -8	second (s)
slug	1.459 390 x E +1	kilogram (kg)
torr (mm Hg, 0^0 C)	1.333 22 x E -1	kilo pascal (kPa)

*The bacquerel (Bq) is the SI unit of radioactivity; 1 Bq = 1 event/s.

**The Gray (GY) is the SI unit of absorbed radiation.

Improved Root Normal Size Distributions for Liquid Atomization

Culbert B. Laney[1]
Engility Corp., 8211 Terminal Rd, Lorton, VA 22079 U.S.A.

Abstract: *This paper identifies two issues with traditional root normal size distributions, which are commonly fitted to experimental results for liquid atomization and sprays. First, while root normal size distributions are typically expressed in terms of mass mean diameter, they do not actually obtain the correct mass mean diameter. The error is usually small but may be significant in some cases. Simple corrective measures are suggested. Second, depending on the chosen form, traditional root normal size distributions may exhibit severe non-physical singularities. An alternative root normal size distribution is suggested that experiences only mild singularities. A literature survey finds six possible parameter choices for root normal size distributions. It is found that these parameter choices provide an adequate fit to a wide variety of experimental data, except possibly for the largest droplets.*

Keywords: Root Normal Size Distribution, Simmons Universal Size Distribution, Spray Atomization, Probability Density Function, Aerosol Size Distribution, Liquid Fragmentation

1. Introduction

First introduced by Tate and Marshall (1953), root normal size distributions are commonly used to describe aerosol size distributions, and appear in most recent textbooks on multiphase flows, atomization, and sprays, e.g., Bayvel and Orzechowski (1993), Liu (2000), Brennan (2005), Crowe (2006), Ashgriz (2011).

Simmons (1977) proposed the best-known root normal size distribution. In particular, the Simmons root normal size distribution has been featured in an extensive series of papers by Dr. Gerard Faeth and his colleagues, e.g., Wu et. al. (1991, 1992 1995); Ruff et. al. (1992); Hsiang and Faeth (1992, 1993); Wu and Faeth (1993), Chou et. al. (1997), Dai et. al. (1998), Sallam et. al. (1999, 2006), Aalberg et. al. (2005), Lee et. al. (2007), Miller et. al. (2008).

As the main advantage of root normal size distributions, the research literature suggests that there are only a limited number of parameter choices. Each such parameter choice is sometimes referred to as a *universal*. Contrast this situation with other distributions, especially those with three or more free parameters, where a small change in the experimental data may lead to a large change in the as-fitted parameters, e.g., Dumouchel (2009), Dumouchel et. al. (2012).

As the main disadvantage of root normal size distributions – as well as all known alternatives – "no single distribution accurately fits even a large fraction of the available drop size data research literature …[which] necessitates trial-and-error use of several distributions to determine which one best fits a particular data set." (Ashgriz, 2011). As one main goal, this paper attempts to clarify how close root normal size distributions, with just a half-a-dozen different parameter settings, can come to fitting a wide variety of experimental data.

[1] E-mail address: Bert.Laney@engilitycorp.com

The research literature offers few mathematical expressions for root normal size distributions. As a second main goal, this paper considers two variants of the root normal size distribution, one common and one rare, with complete mathematical expressions given for both. For example, this treatment provides new algebraic results for the ratio of the mass mean diameter to the Sauter mean diameter, which reveal unexpected sensitivity to an arbitrary minimum droplet size.

Root normal size distributions are often expressed in normalized (self-similar) forms, i.e., with the independent variable divided (and optionally the dependent variable multiplied) by an average droplet size. This paper suggests a way to ensure that root normal size distributions actually obtain the average droplet sizes implied by such normalized forms. This requires sacrificing a free parameter.

Finally, this paper confirms an earlier observation, namely, that the common variant of the root normal size distribution experiences a severe singularity for small droplets. By contrast, this paper finds that the rare variant has only a mild singularity. This observation suggests the use of the rare variant in future work.

Aerosol droplets are typically nearly-spherical; thus aerosol size distributions are usually expressed as functions of droplet diameter. However, certain liquids tend to form highly-distended or stringy fragments including viscoelastic liquids such as silicone oils, non-Newtonian liquids such as starch solutions, and highly-viscous liquids such as thick melts, e.g., Joseph et. al. (1999), Joseph et. al. (2002), Theofanous (2011). Even simple liquids such as water may exhibit irregularly shaped fragments for a brief period of time immediately following an atomization event. Such situations are best described in terms of mass rather than in terms of diameter. Thus this treatment gives expressions both for mass and diameter.

2. Size Distributions and Transformation Conditions

Let D be the droplet diameter and let M be the droplet mass. Then there are eight common ways of expressing aerosol size distributions:

> $F_M(D)$ [$F_M(M)$] is the mass fraction of droplets with diameters [masses] greater than or equal to D [M].
>
> $f_M(D)$ [$f_M(M)$] is the mass fraction of droplets with diameters [masses] in a range dD centered on D divided by dD [dM centered on M divided by dM]
>
> $F(D)$ [$F(M)$] is the number fraction of droplets with diameters [masses] greater than or equal to D [M]
>
> $f(D)$ [$f(M)$] is the number fraction of droplets with diameters [masses] in a range dD centered on D divided by dD [dM centered on M divided by dM]

This list excludes minor variations such as $1 - F_M$, or the use of volume V instead of mass M. The above definitions imply that F_M is monotone decreasing such that $F_M(0) = 1$ and $F_M(\infty) = 0$. In addition, f_M is always non-negative such that:

$$\int_0^\infty f_M(x)dx = 1 \tag{1a}$$

Similarly, the above definitions imply that F is monotone decreasing such that $F(0) = 1$ and $F(\infty) = 0$. In addition, f is always non-negative such that:

$$\int_0^\infty f(x)dx = 1 \tag{1b}$$

In standard probability theory, F is called a *complementary cumulative distribution function* (*CCDF*) and f is called a *probability density function* (*PDF*).

As defined here, the *transformation condition* requires that all eight forms given above have, at most, mild (integrable) singularities. It would not make physical sense for an aerosol size distribution to be well-behaved in one form but to experience severe (non-integrable) singularities in another form. As seen below, traditional root normal size distributions do not obey the transformation condition.

Transforming between the eight different forms given above requires eight different equations. The first of these equations is as follows:

$$M = \rho C D^m \tag{2}$$

where ρ is density, C is a shape factor, and m is the spatial dimension ($1 \le m \le 3$). For classic aerosols with nearly-spherical droplets, $m = 3$. Equation (2) may not apply to certain highly-irregular liquid fragments; this treatment specifically excludes such cases.

The next two transformation equations are as follows:

$$F_M(M) = F_M(D) \tag{3}$$

$$F(M) = F(D) \tag{4}$$

which follow directly from the definitions of the functions involved. The fourth transformation equation is as follows:

$$f_M(x) = \frac{M(x)f(x)}{\int_0^\infty M(x)f(x)dx} \tag{5}$$

This was first introduced by Brown (1989) and Brown and Wohletz (1995); see also Dumouchel (2009). The last four transformation equations are well-known and follow directly from the definitions of the functions involved:

$$F_M(D) = -\int_D^\infty f_M(x)dx\,;\;\; f_M(D) = -\frac{dF_M}{dD} \tag{6}$$

$$F_M(M) = -\int_M^\infty f_M(x)dx\,;\;\; f_M(M) = -\frac{dF_M}{dM} \tag{7}$$

$$F(D) = -\int_D^\infty f(x)dx\,;\;\; f(D) = -\frac{dF}{dD} \tag{8}$$

$$F(M) = -\int_M^\infty f(x)dx\,;\;\; f(M) = -\frac{dF}{dM} \tag{9}$$

3. Average Droplet Sizes and Self-Similarity Conditions

As noted above, average droplet sizes are often used to normalize size distribution functions. The complexity of various mathematical expressions depends on the choice of average. Judging by the complexity of the expressions given later in Sections 5 to 8, the eight size distributions defined above appear to be naturally associated with different average sizes. For example, $F_M(D)$ and $f_M(D)$ are naturally associated with the following two averages:

$$D_{M\,avg} = \int_0^\infty D f_M(D)dD = \frac{\int_0^\infty D^4 f(D)dD}{\int_0^\infty D^3 f(D)dD} \tag{10}$$

$$D'_{M\,avg} = \frac{1}{\int_0^\infty \frac{f_M(D)}{D}dD} = \frac{\int_0^\infty D^3 f(D)dD}{\int_0^\infty D^2 f(D)dD} \tag{11}$$

which are known as the *mass mean diameter (MMD)* and the *Sauter mean diameter (SMD)*, respectively. In the research literature, it is common to see the ratio of these two averages:

$$R_M \equiv \frac{D_{M\,avg}}{D'_{M\,avg}} \tag{12}$$

Notice that $D'_{M\,avg}$ emphasizes small droplets while $D_{M\,avg}$ emphasizes large droplets. As a result, $1 \le R_M \le \infty$ measures aerosol size spread where $R_M = 1$ corresponds to the least possible spread (i.e. monodisperse) while $R_M = \infty$ corresponds to the greatest possible spread.

For another example, $F(D)$ and $f(D)$ are naturally associated with the following two averages:

$$D_{avg} = \int_0^\infty D f(D) dD \tag{13}$$

$$D'_{avg} = \frac{1}{\int_0^\infty \frac{f_M(D)}{D} dD} \tag{14}$$

The former is known as the *count mean diameter (CMD)*. The latter is non-standard and unnamed. As before, one can define a ratio of these two averages:

$$R \equiv \frac{D_{avg}}{D'_{avg}} \tag{15}$$

The observations made earlier about R_M apply equally to R.

As a third example, $F_M(M)$ and $f_M(M)$ are naturally associated with $M_{M\,avg}$ where:

$$M_{M\,avg} = \int_0^\infty M f_M(M) dM = \frac{\int_0^\infty M^2 f(M) dM}{\int_0^\infty M f(M) dM} \tag{16}$$

As a fourth and final example, $F(M)$ and $f(M)$ are naturally associated with M_{avg} where:

$$M_{avg} = \int_0^\infty M f(M) dM \tag{17}$$

When transforming between the eight different size distributions given in Section 2, it is useful to have ratios such as the following:

$$Q = \frac{D_{M\,avg}}{D_{avg}} \tag{18}$$

:

$$S_M \equiv \frac{M_{M\,avg}}{\rho C D_{M\,avg}^m} \tag{19a}$$

$$S \equiv \frac{M_{avg}}{\rho C D_{avg}^m} \tag{19b}$$

Notice that S_M measures skewness, where $S_M = 1$ if the aerosol size distribution is evenly balanced between small and large droplets, e.g., a uniform size distribution. Similar observations apply to *S*.

In the simplest possible case, *self-preserving* or *self-similar* aerosol size distributions can be written in terms of the following ratio:

$$\eta = \frac{M}{M_{M\,avg}}$$

This was first observed by Friedlander and Wang (1966) for populations of droplets that collide with each other; see also Lee et. al. (1984), Spicer and Pratsinis (1996), and Lehtinen and Zachariah (2001). For example, Spicer and Pratsinis (1996) give the following definition: "When the steady-state size distributions scaled by the average particle volume [or mass] collapse onto a single size distribution, this distribution is termed self-preserving."

Using the transformations given in Section 2, self-similar aerosol size distributions can equally well be written in terms of the following ratio:

$$\eta' = \frac{D}{D_{M\,avg}}$$

In fact, as already noted, root normal size distributions are commonly written in such simple self-preserving (normalized) forms. An obvious condition is that, if an aerosol size distribution is written in terms of a given average, it should actually obtain that average. However, as seen below, traditional root normal size distributions do not obey this condition.

4. Modifications for Minimum Droplet Sizes

The vast majority of experiments impose a minimum droplet size $D_{\min}$ or, equivalently, $M_{\min} = \rho C D_{\min}^m$ due to optical resolution or other practical factors. If the minimum droplet size is large enough, the aerosol size distribution should be modified accordingly. For example, F_M should be replaced by $\overline{F}_M$ where $\overline{F}_M(D_{\min}) = 1$ and $\overline{F}_M(\infty) = 0$. This is true if:

$$\overline{F}_M(D) = \frac{F_M(D)}{F_M(D_{\min})} \tag{20}$$

Similarly, f_M should be replaced by $\bar{f}_M$ where:

$$\int_{D_{\min}}^{\infty} \bar{f}_M(D)dD = 1$$

This is true if

$$\bar{f}_M(D) = \frac{f_M(D)}{F_M(D_{\min})} \tag{21}$$

As another example, $D_{M\,avg}$ should be replaced by $\overline{D}_{M\,avg}$ where:

$$\overline{D}_{M\,avg} = \int_{D_{\min}}^{\infty} D\bar{f}_M(D)dD = \frac{1}{F_M(D_{\min})}\int_{D_{\min}}^{\infty} D f_M(D)dD \tag{22}$$

Similarly, $D'_{M\,avg}$ should be replaced by $\overline{D}'_{M\,avg}$ where:

$$\overline{D}'_{M\,avg} = \frac{1}{\int_{D_{\min}}^{\infty} \frac{\bar{f}_M(D)}{D}dD} = \frac{F_M(D_{\min})}{\int_{D_{\min}}^{\infty} \frac{f_M(D)}{D}dD} \tag{23}$$

As a final example, R_M should be replaced by $\overline{R}_M$ where:

$$\overline{R}_M \equiv \frac{\overline{D}_{M\,avg}}{\overline{D}'_{M\,avg}} \tag{24a}$$

or:

$$\overline{R}_M = \frac{1}{F_M(D_{\min})^2}\int_{D_{\min}}^{\infty} D f_M(D)dD \int_{D_{\min}}^{\infty} \frac{1}{D} f_M(D)dD \tag{24b}$$

Alternatively, when $D_{M\,avg}$ is finite while $D'_{M\,avg}$ is not, it is common to see mixed expressions such as the following:

$$\overline{R}_M \equiv \frac{D_{M\,avg}}{\overline{D}'_{M\,avg}} \tag{25}$$

5. Traditional Root Normal Size Distributions (Type I)

The traditional root normal size distribution may be written as follows:

$$f_M(D) = \frac{1}{AD_{M\,avg}} \frac{1}{\sqrt{2\pi\sigma^2}} \frac{1}{\sqrt{D/D_{M\,avg}}} \exp\left[-\frac{1}{2\sigma^2} \left(\sqrt{D/D_{M\,avg}} - a \right)^2 \right] \tag{26}$$

Table 1 recasts this size distribution into eight equivalent forms using the expressions given in Section 2. Unfortunately, there are no known analytical expressions for two of these forms – $F(D)$ and $F(M)$ – meaning they must be determined numerically.

Table 1a. Root normal distributions of Type I expressed in terms of F_M and f_M

$F_M(D) = \frac{1}{A} \operatorname{erfc}\left(\frac{\sqrt{D/D_{M\,avg}} - a}{\sqrt{2}\sigma} \right)$	$F_M(M) = \frac{1}{A} \operatorname{erfc}\left(\frac{(S_M M / M_{M\,avg})^{1/2m} - a}{\sqrt{2}\sigma} \right)$
$f_M(D) = \frac{1}{AD_{M\,avg}} \frac{1}{\sqrt{2\pi\sigma^2}} \times \frac{1}{\sqrt{D/D_{M\,avg}}} \exp\left[-\frac{1}{2\sigma^2} \left(\sqrt{D/D_{M\,avg}} - a \right)^2 \right]$	$f_M(M) = \frac{S_M}{AmM_{M\,avg}} \frac{1}{\sqrt{2\pi\sigma^2}} \times \left(\frac{S_M M}{M_{M\,avg}} \right)^{\frac{1}{2m}-1} \exp\left\{ -\frac{1}{2\sigma^2} \left[\left(\frac{S_M M}{M_{M\,avg}} \right)^{\frac{1}{2m}} - a \right]^2 \right\}$

Table 1b. Root normal distributions of Type I expressed in terms of F and f.

$F(D) = -\int_D^\infty f(x)dx$	$F(M) = -\int_M^\infty f(x)dx$
$f(D) = \frac{1}{BD_{M\,avg}} \frac{1}{\sqrt{2\pi\sigma^2}} \times \left(\frac{D}{D_{M\,avg}} \right)^{-m-1/2} \exp\left[-\frac{1}{2\sigma^2} \left(\sqrt{D/D_{M\,avg}} - a \right)^2 \right]$	$f(M) = \frac{S_M}{BmM_{M\,avg}} \frac{1}{\sqrt{2\pi\sigma^2}} \times \left(\frac{S_M M}{M_{M\,avg}} \right)^{\frac{1}{2m}-2} \exp\left\{ -\frac{1}{2\sigma^2} \left[\left(\frac{S_M M}{M_{M\,avg}} \right)^{\frac{1}{2m}} - a \right]^2 \right\}$

As described in the next section, the traditional root normal size distribution suffers from a mild singularity in f_M but a severe singularity in f at the origin. This singularity has been previously observed by, for example, Babinsky and Sojka (2002), who called it "a gradient catastrophe near zero."

It is convenient to express the properties of the root normal size distribution in terms of the following integral:

$$W_i = \frac{1}{\sqrt{2\pi\sigma^2}} \int_0^\infty x^{i-1/2} \exp\left[-\frac{(\sqrt{x}-a)^2}{2\sigma^2} \right] dx \tag{27}$$

There are analytic expressions for W_i if and only if i is a non-negative integer; see Table 2.

Table 2. Six examples of integrals defined by Equation (27) where erfc is the complementary error function.

i	W_i
0	$\operatorname{erfc}\left(-\frac{a}{\sqrt{2}\sigma} \right)$
1	$(a^2+\sigma^2)\operatorname{erfc}\left(-\frac{a}{\sqrt{2}\sigma} \right) + \frac{2\sigma a}{\sqrt{2\pi}} \exp\left(-\frac{a^2}{2\sigma^2} \right)$
2	$(a^4+6a^2\sigma^2+3\sigma^4)\operatorname{erfc}\left(-\frac{a}{\sqrt{2}\sigma} \right)$ $+(a^2+5\sigma^2)\frac{2\sigma a}{\sqrt{2\pi}} \exp\left(-\frac{a^2}{2\sigma^2} \right)$
3	$(a^6+15a^4\sigma^2+45a^2\sigma^4+15\sigma^6)\operatorname{erfc}\left(-\frac{a}{\sqrt{2}\sigma} \right)$ $+(a^4+14a^2\sigma^2+33\sigma^4)\frac{2\sigma a}{\sqrt{2\pi}} \exp\left(-\frac{a^2}{2\sigma^2} \right)$
4	$(a^8+28a^6\sigma^2+210a^4\sigma^4+420a^2\sigma^6+105\sigma^8)\operatorname{erfc}\left(-\frac{a}{\sqrt{2}\sigma} \right)$ $+(a^6+27a^4\sigma^2+185a^2\sigma^4+279\sigma^6)\frac{2\sigma a}{\sqrt{2\pi}} \exp\left(-\frac{a^2}{2\sigma^2} \right)$
6	$(a^{12}+66\,a^{10}\sigma^2+1485\,a^8\sigma^4+13860\,a^6\sigma^6+51975\,a^4\sigma^8$ $+62370a^2\sigma^{10}+10395\sigma^{12})\operatorname{erfc}\left(-\frac{a}{\sqrt{2}\sigma} \right)$ $+(a^{10}+65\,a^8\sigma^2+1422\,a^6\sigma^4+12558\,a^4\sigma^6$ $+41685a^2\sigma^8+35685\sigma^{10})\frac{2\sigma a}{\sqrt{2\pi}} \exp\left(-\frac{a^2}{2\sigma^2} \right)$

By Equation (1):

$$A = W_0 \tag{28}$$

$$B = W_{-m} \tag{29}$$

By Equations (12), (15), and (18):

$$R_M = \frac{W_{-1} W_1}{W_0^2} \tag{30}$$

$$R = \frac{W_{-m+1} W_{-m-1}}{W_{-m}^2} \tag{31}$$

$$Q = \frac{W_1}{W_0} \frac{W_{-m}}{W_{-m+1}} \tag{32}$$

Because of the singularity at the origin, Equations (29) to (32) require imposing a minimum droplet size $D_{\min}$. The minimum droplet size must be applied to those W_i with a negative index i and, optionally, to all W_i. In other words, B should be replaced by $\overline{B}$, R_M should be replaced by $\overline{R}_M$, R should be replaced by $\overline{R}$, and Q should be replaced by $\overline{Q}$ as described in Section 4.

Figure 1 shows how $\overline{R}_M$ depends on $D_{\min}$ and σ. Notice that $\overline{R}_M$ is relatively insensitive to the arbitrary choice of $D_{\min}$ for $0 < \sigma < 0.2$. However, $\overline{R}_M$ may be extremely sensitive to $D_{\min}$ for larger σ. It is a common practice in the research literature to specify $\overline{R}_M$ rather than σ. However, this may be somewhat confusing given that $\overline{R}_M$ depends on an arbitrary $D_{\min}$, at least for $\sigma > 0.2$ For most cases seen in the research literature, $D_{\min} / D_{M\,avg}$ is somewhere between 0.1 and 0.2. Figure 2 shows that $\overline{R}_M$ may vary substantially over this range when $\sigma > 0.2$.

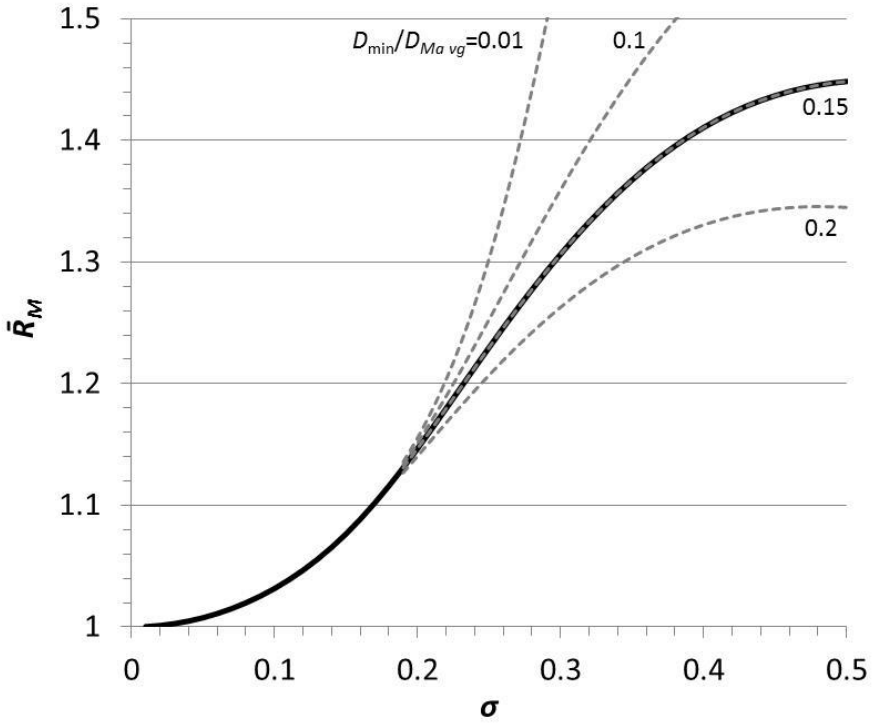

Figure 1. The ratio R_M for traditional (Type I) root normal size distributions with a=1.

If $F_M(D)$ and $f_M(D)$ are self-similar, then $D_{M\,avg}$ in Table 1a must agree with $D_{M\,avg}$ as defined by Equation (10). This is true if:

$$W_0 = W_1 \tag{33}$$

According to Table 2, this can be written as follows:

$$\sigma^2 + a^2 + \frac{2\sigma a}{\sqrt{2\pi}} \frac{\exp(-a^2/2\sigma^2)}{\operatorname{erfc}(-a/\sqrt{2}\sigma)} = 1$$

This is approximately true if:

$$a = \sqrt{1-\sigma^2} \tag{34}$$

Equations (33) and (34) have not appeared in the research literature before. Rather, past treatments assumed $a = 1$. Figure 2 compares Equations (33), Equations (34), and the traditional choice of $a = 1$.

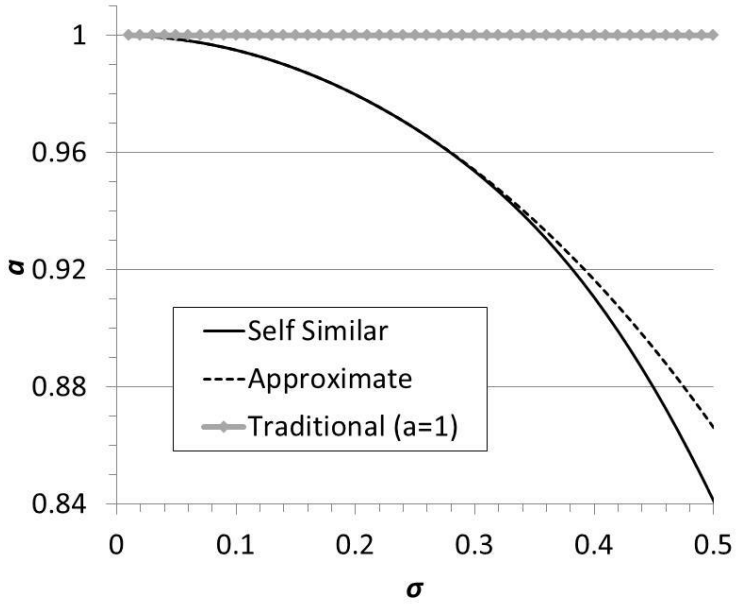

Figure 2. The relationship between parameters *a* and *σ* required to ensure that traditional (Type I) root normal size distributions have the correct count mean diameter. In the legend, 'self similar' refers to Equation (33) while 'approximate' refers to Equation (34).

Figure 3 illustrates the effects of changing a. More specifically, Figure 3 compares the effects of using a fixed value of $a = 1$ versus Equation (33). In this example, the choice $a = 1$ results in mass mean diameter that is about 6% too large while the choice $a = 0.9708$ results in the correct mass mean diameter.

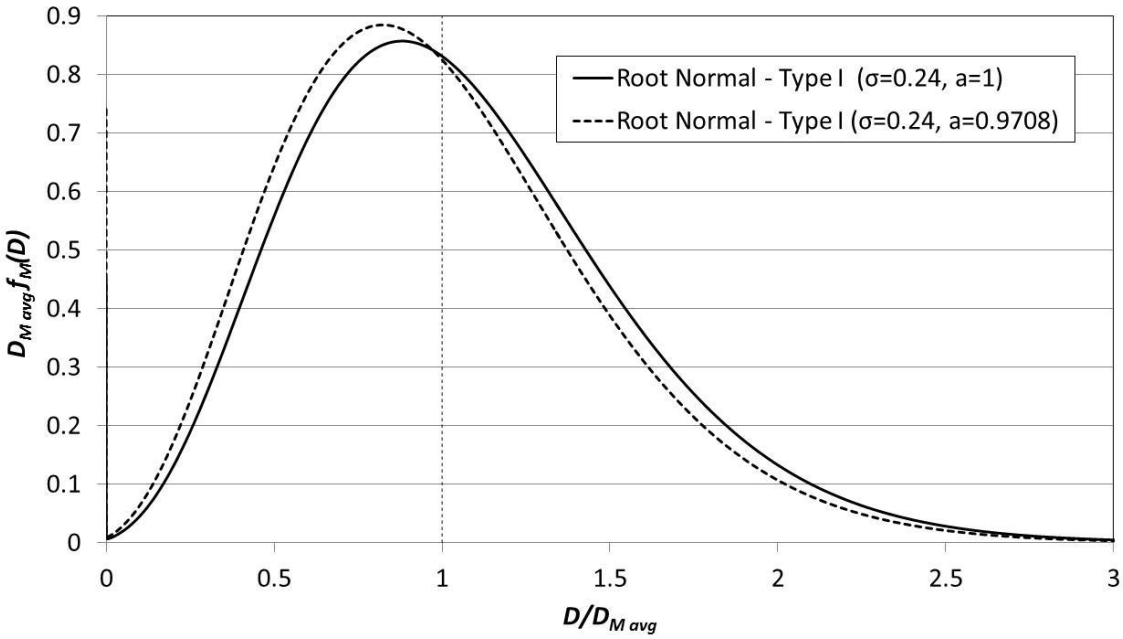

Figure 3. Traditional (Type I) root normal size distributions with *σ*=0.24 and *a*=1 vs. *a*=0.9708. The latter value of *a* was chosen using Equation (33) to ensure the correct mass mean diameter.

If $F_M(M)$ and $f_M(M)$ are self-similar, then $M_{M\,avg}$ in Table 1a must agree with $M_{M\,avg}$ as defined by Equation (19). This is true if:

$$S_M = \frac{W_m}{W_0} \tag{35}$$

For example, if $m = 3$ and Equation (33) is exactly true, then Equation (35) becomes:

$$S_M = a^4 + 14a^2\sigma^2 + 33\sigma^4 - 2a^2\sigma^4 - 18\sigma^6$$

6. Variant of Traditional Root Normal Size Distributions (Type IB)

Suppose the traditional (Type I) root normal size distribution is modified as follows:

$$f_M(D) = \frac{1}{AD_{avg}} \frac{1}{\sqrt{2\pi\sigma^2}} \frac{1}{\sqrt{D/D_{avg}}} \exp\left[-\frac{1}{2\sigma^2} (\sqrt{D/D_{avg}} - a)^2 \right] \tag{36}$$

Notice that Equation (36) is the same as Equation (26), except that the mass mean diameter $D_{M\,avg}$ has been replaced by the count mean diameter D_{avg}. Equation (36) can be recast in eight different forms. The results are identical to those given earlier in Table 1 after replacing $D_{M\,avg}$ by D_{avg}, $M_{M\,avg}$ by M_{avg}, and S_M by *S*.

Most properties of Equation (36) are exactly the same as those of Equation (26). In particular, Equations (28) to (32) are the same as before. Only the self-similarity conditions change to become:

$$W_{-m} = W_{-m+1} \tag{37}$$

$$S = \frac{W_0}{W_{-m}} \tag{38}$$

Unlike Equations (33) and (35), Equations (37) and (38) require imposing a minimum droplet size $D_{\min}$. This extra complication makes Type IB root normal size distributions unattractive.

7. Alternative Root Normal Size Distributions (Type II)

Consider the following alternative root normal size distribution:

$$f(D) = \frac{1}{AD_{M\,avg}} \frac{1}{\sqrt{2\pi\sigma^2}} \frac{1}{\sqrt{D/D_{M\,avg}}} \exp\left[-\frac{1}{2\sigma^2} (\sqrt{D/D_{M\,avg}} - a)^2 \right] \tag{39}$$

Notice that Equation (39) is identical to Equation (26) except that f_M has been replaced by f. While this alternative root normal distribution has been mentioned in the research literature before, e.g., Crowe (2006), its properties have never been well-described. Table 3 recasts this size distribution into eight equivalent forms using the expressions given in Section 2.

As specific examples, Table 4 gives expressions for F_M and f_M for $m = 1$, 2, and 3. There are analytical expressions for F_M if and only if m is an integer.

As seen in Figure 4a, when expressed in terms of f_M, the traditional root normal size distribution has a mild singularity at the origin while the alternative root normal size distribution has no singularity. As seen in Figure 4b, when expressed in terms of f, the traditional root normal size distribution has a severe singularity at the origin while the alternative root normal size distribution has only a mild singularity. In other words, the alternative root normal size distribution satisfies the transformation condition proposed in Section 2 while the traditional root normal size distribution does not.

Table 3a. Root normal distributions of Type IIA expressed in terms of *F* and *f*.

$$F(D)=\frac{1}{A}\operatorname{erfc}\left(\frac{\sqrt{D/D_{M\,avg}}-a}{\sqrt{2}\sigma}\right)$$	$$F(M)=\frac{1}{A}\operatorname{erfc}\left(\frac{(S_M M/M_{M\,avg})^{1/2m}-a}{\sqrt{2}\sigma}\right)$$
$$f(D)=\frac{1}{AD_{M\,avg}}\frac{1}{\sqrt{2\pi\sigma^2}}\times \frac{1}{\sqrt{D/D_{M\,avg}}}\exp\left[-\frac{1}{2\sigma^2}(\sqrt{D/D_{M\,avg}}-a)^2\right]$$	$$f(M)=\frac{S_M}{AmM_{M\,avg}}\frac{1}{\sqrt{2\pi\sigma^2}}\times \left(\frac{S_M M}{M_{M\,avg}}\right)^{\frac{1}{2m}-1}\exp\left\{-\frac{1}{2\sigma^2}\left[\left(\frac{S_M M}{M_{M\,avg}}\right)^{\frac{1}{2m}}-a\right]^2\right\}$$

Table 3b. Root normal distributions of Type IIA expressed in terms of F_M and f_M for arbitrary *m*.

$$F_M(D)=-\int_D^\infty f_M(x)dx$$	$$F_M(M)=-\int_M^\infty f_M(x)dx$$
$$f_M(D)=\frac{1}{BD_{M\,avg}}\frac{1}{\sqrt{2\pi\sigma^2}}\times \left(\frac{D}{D_{M\,avg}}\right)^{m-1/2}\exp\left[-\frac{1}{2\sigma^2}(\sqrt{D/D_{M\,avg}}-a)^2\right]$$	$$f_M(M)=\frac{S_M}{BmM_{M\,avg}}\frac{1}{\sqrt{2\pi\sigma^2}}\times \left(\frac{S_M M}{M_{M\,avg}}\right)^{\frac{1}{2m}}\exp\left\{-\frac{1}{2\sigma^2}\left[\left(\frac{S_M M}{M_{M\,avg}}\right)^{\frac{1}{2m}}-a\right]^2\right\}$$

Table 4a. Root normal distributions of Type IIA expressed in terms of F_M and f_M for m = 1

$$F_M(D) = \frac{1}{B}(a^2+\sigma^2)\text{erfc}\left(\frac{\sqrt{D/D_{M\,avg}}-a}{\sqrt{2}\sigma}\right) + \frac{2\sigma}{\sqrt{2\pi}B}\left(\sqrt{D/D_{M\,avg}}+a\right)\exp\left[-\frac{1}{2\sigma^2}(\sqrt{D/D_{M\,avg}}-a)^2\right]$$	$$F_M(M) = \frac{1}{B}(a^2+\sigma^2)\text{erfc}\left(\frac{\sqrt{S_M M/M_{M\,avg}}-a}{\sqrt{2}\sigma}\right) + \frac{2\sigma}{\sqrt{2\pi}B}\left(\sqrt{S_M M/M_{M\,avg}}+a\right)\exp\left[-\frac{1}{2\sigma^2}(\sqrt{S_M M/M_{M\ldots avg}}-a)^2\right]$$
$$f_M(D) = \frac{1}{BD_{M\,avg}}\frac{1}{\sqrt{2\pi\sigma^2}}\sqrt{D/D_{M\,avg}}\exp\left[-\frac{(\sqrt{D/D_{M\,avg}}-a)^2}{2\sigma^2}\right]$$	$$f_M(M) = \frac{S_M}{BM_{M\,avg}}\frac{1}{\sqrt{2\pi\sigma^2}}\sqrt{S_M M/M_{M\,avg}}\exp\left[-\frac{(\sqrt{S_M M/M_{M\,avg}}-a)^2}{2\sigma^2}\right]$$

Table 4b. Root normal distributions of Type IIA expressed in terms of F_M and f_M for m = 2

$$F_M(D) = \frac{1}{B}(a^4+6a^2\sigma^2+3\sigma^4)\text{erfc}\left(\frac{(D/D_{M\,avg})^{1/2}-a}{\sqrt{2}\sigma}\right) + \frac{2\sigma}{\sqrt{2\pi}B}\left[\left(\frac{D}{D_{M\,avg}}\right)^{\frac{3}{2}} + a\frac{D}{D_{M\,avg}} + (a^2+3\sigma^2)\left(\frac{D}{D_{M\,avg}}\right)^{\frac{1}{2}} + a^3+5a\sigma^2\right]\exp\left(-\frac{((D/D_{M\,avg})^{1/2}-a)^2}{2\sigma^2}\right)$$	$$F_M(M) = \frac{1}{B}(a^4+6a^2\sigma^2+3\sigma^4)\text{erfc}\left(\frac{(S_M M/M_{M\,avg})^{1/4}-a}{\sqrt{2}\sigma}\right) + \frac{2\sigma}{\sqrt{2\pi}B}\left[\left(\frac{S_M M}{M_{M\,avg}}\right)^{\frac{3}{4}} + a\left(\frac{S_M M}{M_{M\,avg}}\right)^{\frac{1}{2}} + (a^2+3\sigma^2)\left(\frac{S_M M}{M_{M\,avg}}\right)^{\frac{1}{4}} + a^3+5a\sigma^2\right]\exp\left(-\frac{((S_M M/M_{M\,avg})^{1/4}-a)^2}{2\sigma^2}\right)$$
$$f_M(D) = \frac{1}{BD_{M\,avg}}\frac{1}{\sqrt{2\pi\sigma^2}}\left(\frac{D}{D_{M\,avg}}\right)^{\frac{3}{2}}\exp\left\{-\frac{1}{2\sigma^2}\left[\left(\frac{D}{D_{M\,avg}}\right)^{\frac{1}{2}}-a\right]^2\right\}$$	$$f_M(M) = \frac{S_M}{2BM_{M\,avg}}\frac{1}{\sqrt{2\pi\sigma^2}}\left(\frac{S_M M}{M_{M\,avg}}\right)^{\frac{1}{4}}\exp\left\{-\frac{1}{2\sigma^2}\left[\left(\frac{S_M M}{M_{M\,avg}}\right)^{\frac{1}{4}}-a\right]^2\right\}$$

Table 4c. Root normal distributions of Type IIA expressed in terms of F_M and f_M for m = 3

$$F_M(D) = \frac{1}{B}(a^6 + 15a^4\sigma^2 + 45a^2\sigma^4 + 15\sigma^6) \times \operatorname{erfc}\left\{\frac{1}{\sqrt{2}\sigma}\left[\left(\frac{D}{D_{M\,avg}}\right)^{1/2} - a\right]\right\} + \frac{2\sigma}{\sqrt{2\pi}B}\left[\left(\frac{D}{D_{M\,avg}}\right)^{\frac{5}{2}} + a\left(\frac{D}{D_{M\,avg}}\right)^{2} + (a^2 + 5\sigma^2)\left(\frac{D}{D_{M\,avg}}\right)^{\frac{3}{2}} + (a^3 + 9a\sigma^2)\frac{D}{D_{M\,avg}} + (a^4 + 12a^2\sigma^2 + 15\sigma^4)\left(\frac{D}{D_{M\,avg}}\right)^{\frac{1}{2}} + a^5 + 14a^3\sigma^2 + 33a\sigma^4\right] \exp\left\{-\frac{1}{2\sigma^2}\left[\left(\frac{D}{D_{M\,avg}}\right)^{\frac{1}{2}} - a\right]^2\right\}$$	$$F_M(M) = \frac{1}{B}(a^6 + 15a^4\sigma^2 + 45a^2\sigma^4 + 15\sigma^6) \times \operatorname{erfc}\left\{\frac{1}{\sqrt{2}\sigma}\left[\left(\frac{S_M M}{M_{M\,avg}}\right)^{1/6} - a\right]\right\} + \frac{2\sigma}{\sqrt{2\pi}B}\left[\left(\frac{S_M M}{M_{M\,avg}}\right)^{\frac{5}{6}} + a\left(\frac{S_M M}{M_{M\,avg}}\right)^{\frac{2}{3}} + (a^2 + 5\sigma^2)\left(\frac{S_M M}{M_{M\,avg}}\right)^{\frac{1}{2}} + (a^3 + 9a\sigma^2)\left(\frac{S_M M}{M_{M\,avg}}\right)^{\frac{1}{3}} + (a^4 + 12a^2\sigma^2 + 15\sigma^4)\left(\frac{S_M M}{M_{M\,avg}}\right)^{\frac{1}{6}} + a^5 + 14a^3\sigma^2 + 33a\sigma^4\right] \exp\left\{-\frac{1}{2\sigma^2}\left[\left(\frac{S_M M}{M_{M\,avg}}\right)^{\frac{1}{6}} - a\right]^2\right\}$$
$$f_M(D) = \frac{1}{BD_{avg}}\frac{1}{\sqrt{2\pi\sigma^2}}\left(\frac{D}{D_{M\,avg}}\right)^{\frac{5}{2}} \exp\left\{-\frac{1}{2\sigma^2}\left[\left(\frac{D}{D_{M\,avg}}\right)^{\frac{1}{2}} - a\right]^2\right\}$$	$$f_M(M) = \frac{S_M}{3BM_{M\,avg}}\frac{1}{\sqrt{2\pi\sigma^2}}\left(\frac{S_M M}{M_{M\,avg}}\right)^{\frac{1}{6}} \exp\left\{-\frac{1}{2\sigma^2}\left[\left(\frac{S_M M}{M_{M\,avg}}\right)^{\frac{1}{6}} - a\right]^2\right\}$$

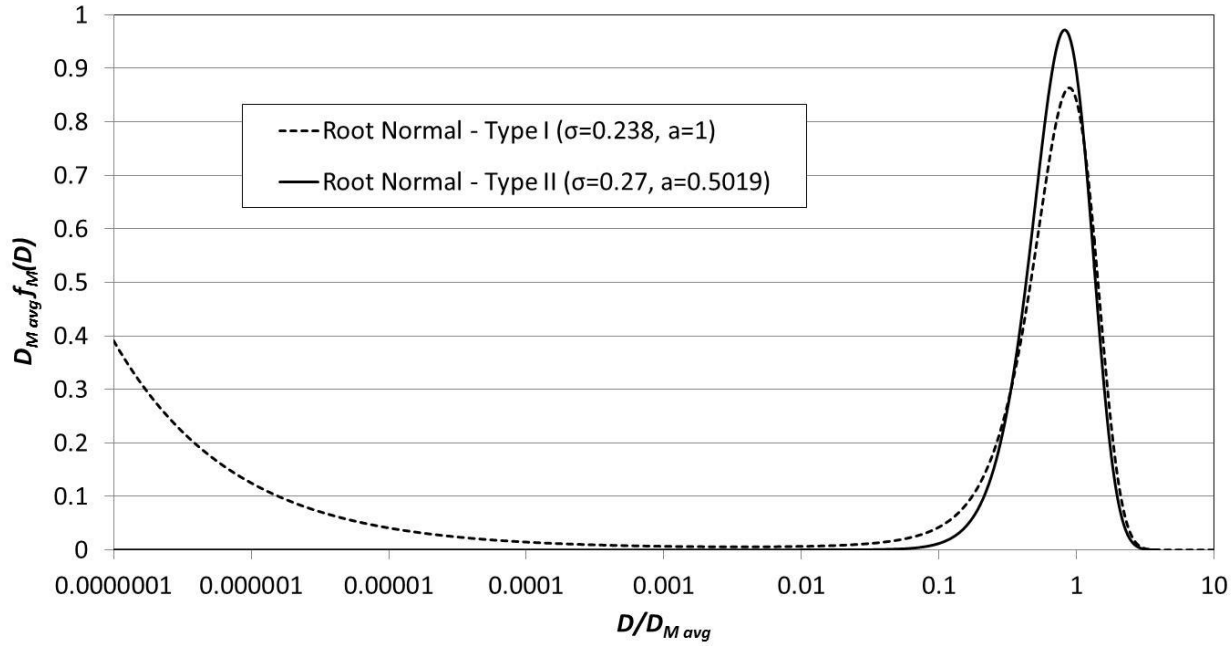

(a.) $f_M(D)$ for Type I vs. Type II root normal size distributions in a linear-log plane.

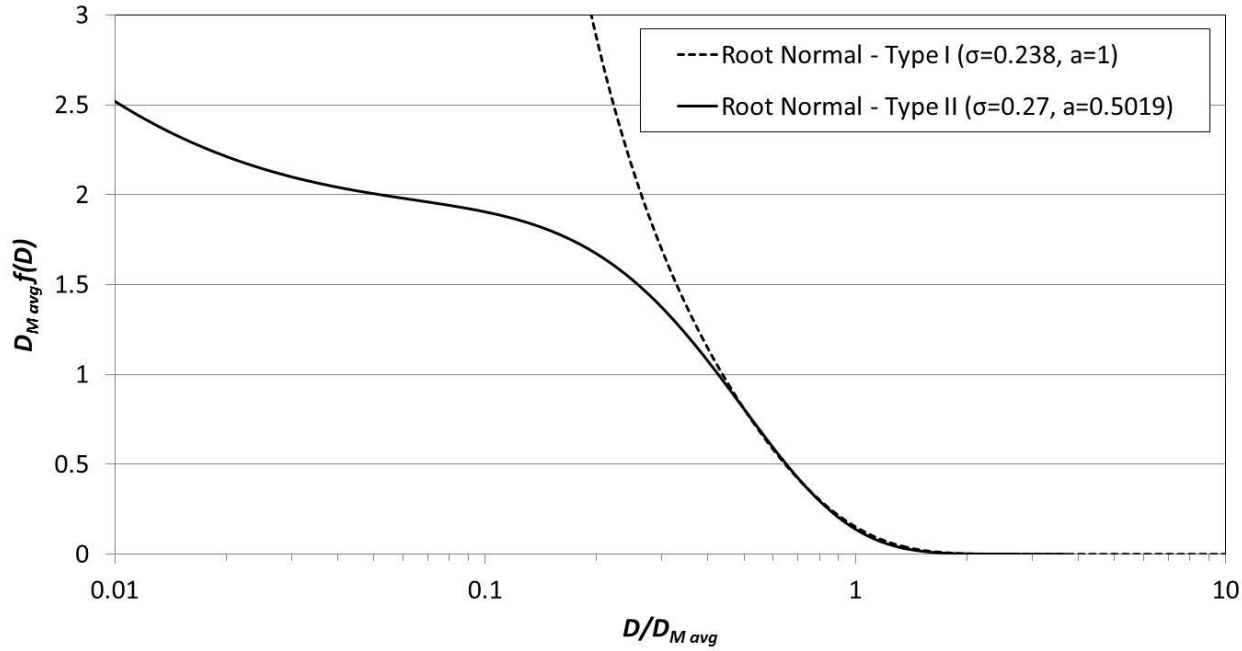

(b.) $f(D)$ for Type I vs. Type II root normal size distributions in a linear-log plane.

Figure 4. The Type I root normal size distribution experiences a mild singularity in $f_M(D)$ and a severe singularity in $f(D)$. The Type II root normal size distribution does not experience any singularity in $f_M(D)$ and experiences only a mild singularity in $f(D)$. The parameter settings for the Type I distribution are σ=0.238 and a=1. The parameter settings for the Type II distribution are σ=0.27, a=0.5019, and m=3 where the value of a is chosen to ensure the correct mass mean diameter.

By Equation (1):

$$A = W_0 \tag{40}$$

$$B = W_m \tag{41}$$

By Equations (12), (15), and (18):

$$R_M = \frac{W_{m-1} W_{m+1}}{W_m^2} \tag{42}$$

$$R = \frac{W_{-1} W_1}{W_0^2} \tag{43}$$

$$Q = \frac{W_0}{W_1} \frac{W_{m+1}}{W_m} \tag{44}$$

Equation (43) requires imposing a minimum droplet size $D_{\min}$. This minimum droplet size should be applied to W_{-1} and, optionally, W_0 and W_1. In other words, R should be replaced by $\overline{R}$ as described in Section 4.

Figure 5 shows R_M as a function of σ. Unlike Type I distributions, Type II distributions have a one-to-one analytical relationship between R_M and σ. Notice that the Type II results agree well with the Type I results when the latter has $D_{\min} / D_{M\,avg} = 0.15$.

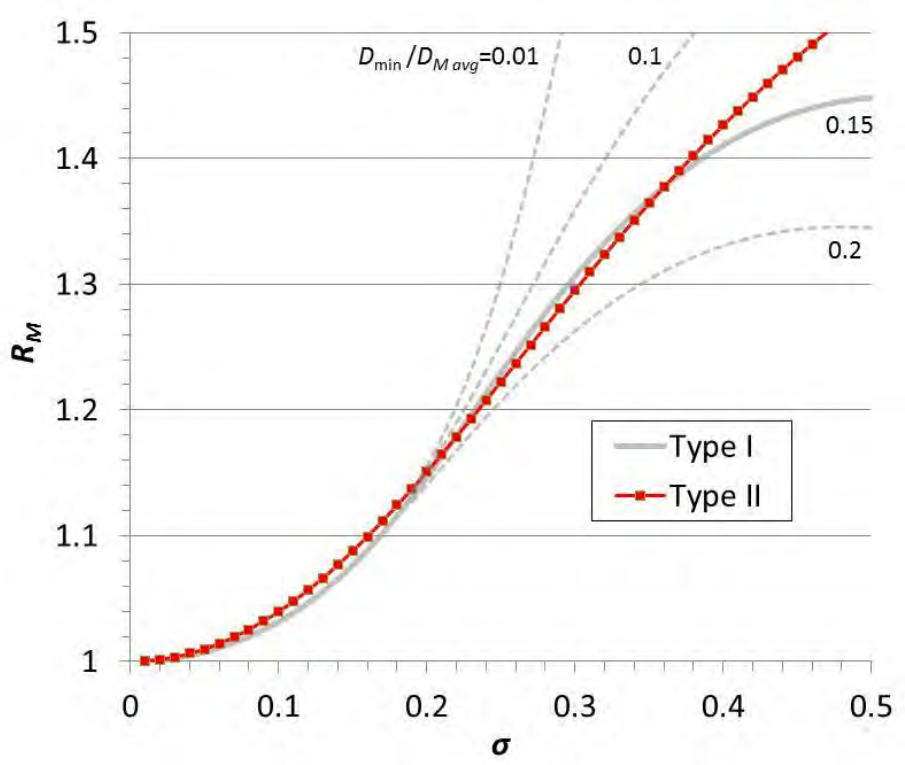

Figure 5. The ratio R_M for alternative (Type II) root normal size distributions with a chosen to ensure self-similarity. For comparison, results for traditional (Type I) root normal distributions with a=1 are also shown.

If $F_M(D)$ and $f_M(D)$ are self-similar, then $D_{M\,avg}$ in Table 3 must agree with $D_{M\,avg}$ as defined by Equation (10). This is true if:

$$W_m = W_{m+1} \tag{45}$$

Figure 6 shows how a varies with σ per Equation (45).

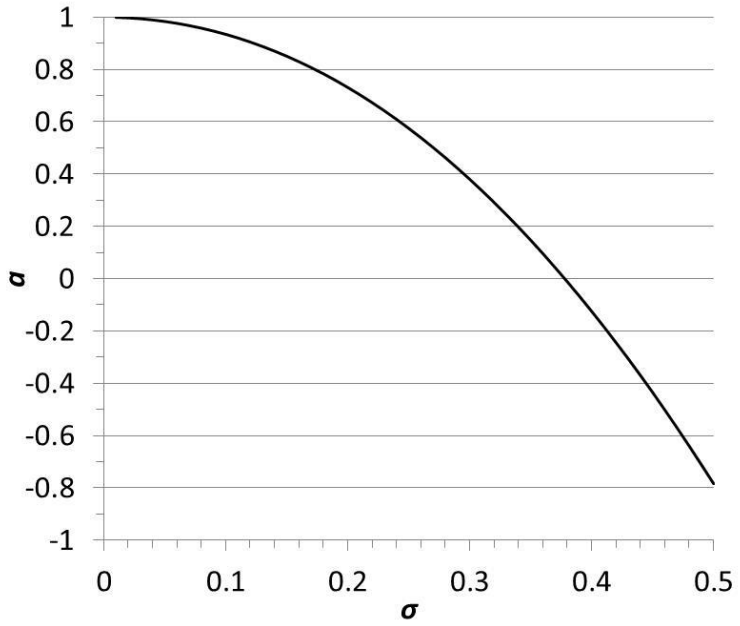

Figure 6. The relationship between parameters *a* and *σ* required to ensure that Type II root normal size distributions have the correct mass mean diameter. This assumes that *m*=3. This is a plot of Equation (45).

If $F_M(M)$ and $f_M(M)$ are self-similar, then $M_{M\,avg}$ in Table 3 must agree with $M_{M\,avg}$ as defined by Equation (19). This is true if:

$$S_M = \frac{W_{2m}}{W_m} \tag{46}$$

8. Variant of Alternative Root Normal Size Distributions (Type IIB)

Suppose the alternative (Type II) root normal size distribution is modified as follows:

$$f(D) = \frac{1}{AD_{avg}} \frac{1}{\sqrt{2\pi\sigma^2}} \frac{1}{\sqrt{D/D_{avg}}} \exp\left[-\frac{1}{2\sigma^2} (\sqrt{D/D_{avg}} - a)^2 \right] \tag{47}$$

Notice that Equation (47) is the same as Equation (39), except that the mass mean diameter $D_{M\,avg}$ has been replaced by the count mean diameter D_{avg}. Equation (47) can be recast in the usual eight forms. The results are identical to those given earlier in Table 3 after replacing $D_{M\,avg}$ by D_{avg}, $M_{M\,avg}$ by M_{avg}, and S_M by S.

Most properties of Equation (47) are exactly the same as those of Equation (39). In particular, Equations (40) to (44) are the same as before. Only the self-similarity conditions change to become:

$$W_0 = W_1 \tag{48}$$

$$S = \frac{W_m}{W_0} \tag{49}$$

Notice that Equations (48) and (49) for Type IIB distributions are the same as Equations (33) and (35) for Type I distributions, after replacing S_M by S. Thus the earlier discussion applies here, including Figures 2 and 3. .

Figure 7 gives an example showing that, with the right parameter choice, Type II and IIB root normal size distributions are nearly identical. Notice that the Type IIB distribution is plotted as $Qf_M(QD)$. As their main advantage, Type IIB distributions have somewhat simpler self-similarity conditions than Type II distributions.

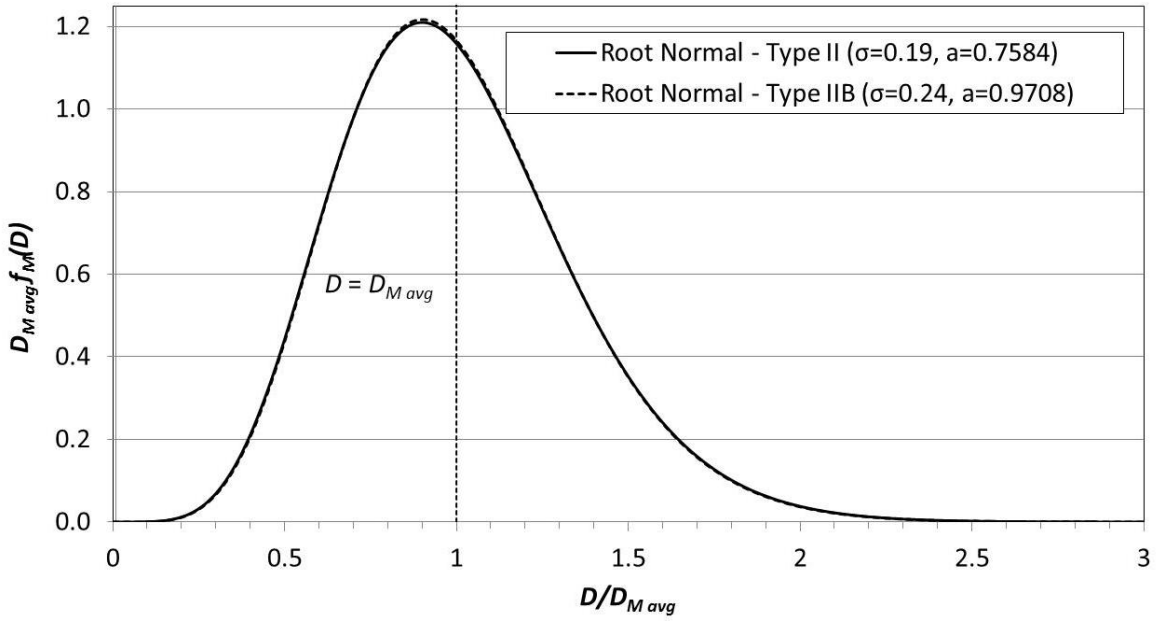

Figure 7. An example of Type II vs. Type IIB root normal size distributions for *m*=3. The parameter *a* in both cases is chosen to ensure self-similarity, i.e., the Type II has the correct MMD and the Type IIB has the correct CMD.

9. Experimental Evidence

Table 5 lists six root normal size distributions found in a literature search. Each reference given in Table 5 typically provides three root normal size distributions -- an upper bound, a lower bound, and an average – to describe anywhere between four and 2,000 separate tests. For the references marked by an asterisks, the given root normal size distribution is a lower bound to multiple sets of test data. For the remainder, the given root normal size distribution is an average of multiple sets of test data.

Table 5. Six examples of traditional (Type I) root normal size distributions found in the research literature. The values given in bold are specified in the original reference. The other values are derived. All root normals are averages of multiple sets of test data except where noted.

	σ	a	$\overline{R}_M$	**Reference(s)**
1	0.081	**1**	**1.02**	Chou & Faeth (1998) (*)
2	0.11	**1**	**1.04**	Sallam et. al. (2006) (*)
3	0.17	**1**	**1.10**	Wu et. al. (1991) (*); Sallam et. al. (2006)
4	**0.20**	**1**	1.15	Empie et. al. (1993, 1995, 1997)
5	**0.238**	**1**	**1.20**	Simmons (1977); Wu et. al. (1991); Ruff et. al. (1992); etc.
6	**0.286**	**1**	1.5 (†)	Speilbauer et. al. (1989); Adams et. al. (1990); Loebker & Empie (2001)

(†) Highly sensitive to the choice of minimum droplet size.

(*) Lower bound to multiple sets of test data in terms of $\overline{R}_M$.

In general, the curve fits in Table 5 were derived using a traditional procedure that involves, first, transforming the test data into a plane in which the presumed size distribution is linear and, second, using least squares to estimate the slope. In the case of power laws, Clauset et. al. (2009) has criticized this approach as follows: "*commonly used methods for analyzing power-law data, such as least-squares fitting, can produce substantially inaccurate estimates of parameters … Even in cases where such methods return accurate answers they are still unsatisfactory because they give no indication of whether the data obey a power law at all*." The same criticism applies in general, including to root normal size distributions. However, regardless of such concerns, some of the root normal fits listed in Table 5 – especially Simmons universal – have been successfully applied to a wide variety of tests for decades.

Pimentel et. al. (2010) compiled 42 test results for spray atomization, including both their own original results and those found in a literature survey done by Paloposki (1994). This is a neutral source of test data, in the sense that most of it has not been previously fitted by root normal size distributions. As shown in Table 6, all of these test results can be reasonably well-fitted by one of the six root normal size distributions listed in Table 5, with the exception of three tests due to Bhatia et. al. (1988), which are omitted.

The size distributions given in Table 6 were chosen to minimize the average error in four different views, namely, $f_M(D)$ in the linear-linear plane, $f_M(D)$ in the log-log plane, $f(D)$ in the linear-linear plane, and $f(D)$ in the log-log plane. In essence, each view implies a different weighting on the error. In most cases, a maximum droplet size was imposed prior to choosing the size distribution. This affects quantities such as the mass mean diameter. The maximum droplet size addresses three issues: first, it balances out the effects of minimum droplet sizes inherent to most tests; second, it avoids random variations caused by small samples of large droplets seen in some tests; and, third, it avoids divergence from root normal size distributions for the largest droplets seen in some tests.

Table 6. Experimental results for spray atomization given by Pimentel et. al. (2010). As indicated in the first and second columns, all results can be reasonably well-fitted by one of the root normal size distributions listed in Table 5, except for those from Bhatia et. al . (1988), which are omitted.

	σ	Reference(s)	Liquid	Spray System	No.	%
1	0.081	Pimentel et. al. (2010)	Jet Fuel	'Delavan'	3	7.8
2	0.11	Pimentel et. al. (2010) ″ ″	Jet Fuel ″ ″	'Bosch' 'BETE' 'Delavan'	4 9 1	35.9
3	0.17	Pimentel et. al. (2010) Paloposki & Fagerholm (1986) Li & Tankin (1987) Tishkoff (1979)	(unknown) Fuel Oil Water Water	'LaVision' Hollow Cone Solid Cone Hollow Cone	3 5 4 2	35.9
4	0.20	Turner & Moulton (1953)	β-naphthol	Swirl Jet	4	10.2
5	0.238	Tate & Olson (1962) Houghton (1941)	Water (unknown)	Solid, Hollow Cone (unknown)	3 1	10.2
6	0.286	-	-	-	0	0

The following subsections review the experimental evidence found in the research literature for each of the size distributions listed in Table 5. In addition, the following subsections compare test data to the chosen root normal size distributions for each case listed in Table 6.

9.1 Experimental Evidence for σ = 0.081

As an example, Chou and Faeth (1998) studied aerodynamic breakup of water and glycerol-water droplets. They found that bag-type breakup, excluding the basal ring, led to Type I root normal size distributions with a lower bound of $\overline{R}_M \approx 1.02$, an upper bound of $\overline{R}_M \approx 1.10$, and an average of $\overline{R}_M \approx 1.04$. The two tests with the most glycerol (42%, 63%) did not consistently obtain the lower bound, upper bound, or average. However, the two tests with the least glycerol (0%, 21%) approximately obtained the lower bound of $\overline{R}_M \approx 1.02$ or, equivalently, $\sigma \approx 0.081$ and $a = 1$.

As another example, Figure 8 compares Type I and II root normal distributions against experimental data obtained by Pimentel et. al. (2010) using several different Delavan atomizers. The Type I and II distributions are essentially identical. The root normal distributions only agree with the experimental results for the smallest droplets. The larger droplets appear to approximately obey a power law rather than a root normal distribution, as indicated by linearity in the log-log plane.

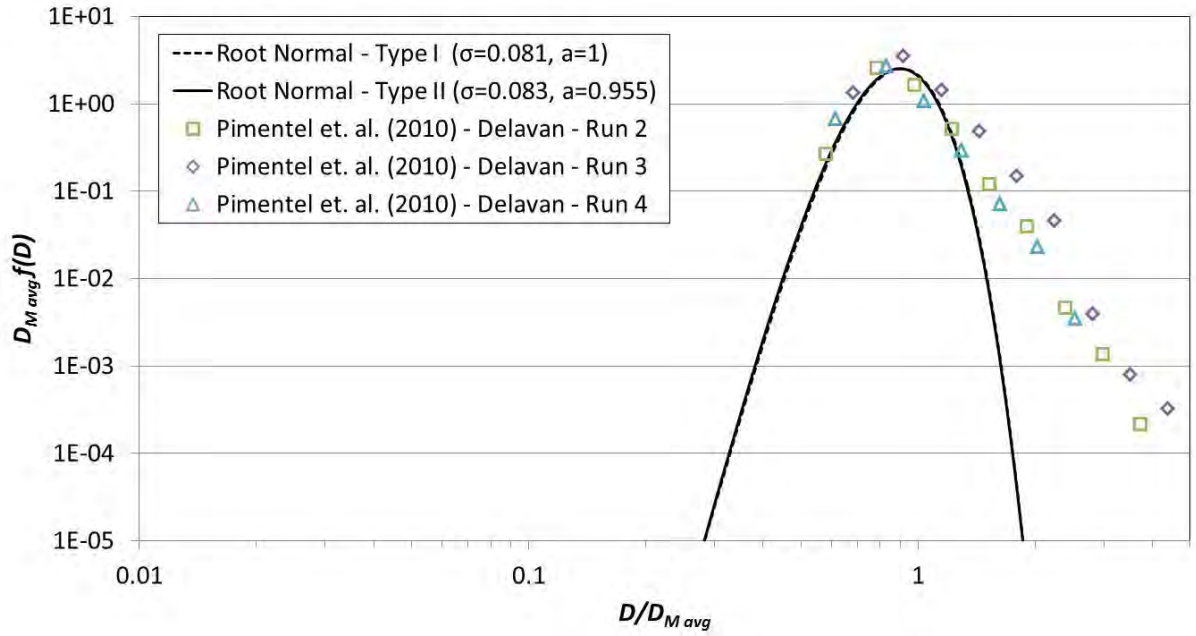

(a.) Log-log plane

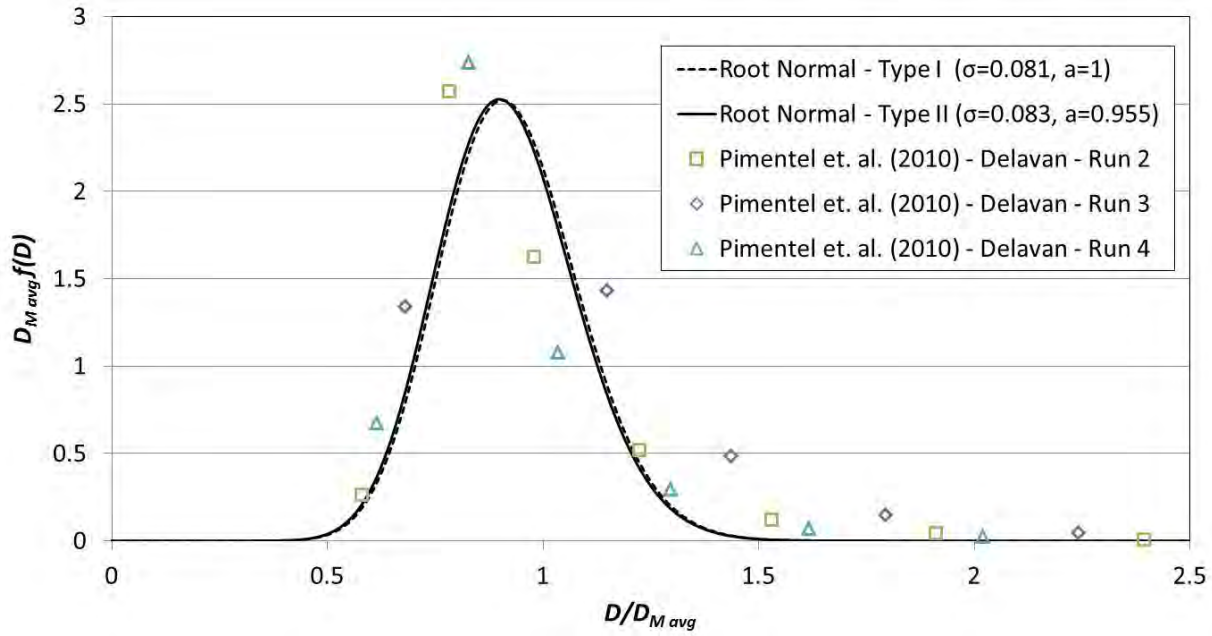

(b.) Linear-linear plane

Figure 8. Type I vs. Type II root normal distributions compared to experimental results obtained by Pimentel et. al. (2010) using Delavan atomizers.

9.2 Experimental Evidence for σ = 0.11

As an example, Sallam et. al. (2006) studied primary breakup of round aerated jets of water, ethyl alcohol, and 79% glycerol solutions in supersonic crossflows. They found Type I root normal size distributions with a lower bound of $\overline{R}_M \approx 1.04$ and an upper bound of $\overline{R}_M \approx 1.10$. Two of the five tests were somewhere between the upper and lower bounds. One of the five tests approximately obtained the upper bound. Two of the five tests approximately obtained the lower bound; more specifically, water and glycerol with jet diameters of 0.5mm approximately obtained $\overline{R}_M \approx 1.04$ or, equivalently, $\sigma \approx 0.11$ and $a = 1$.

As another example, Figure 9 compares Type I and II root normal distributions against experimental data obtained by Pimentel et. al. (2010) using a common rail Bosch system and a BETE XA-PR200 nozzle. The Type I and II distributions are essentially identical. The Type I and II distributions agree reasonably well with the experimental results, except for the largest droplets. As before, in the experiments, the largest droplets appear to approximately obey a power law rather than a root normal distribution.

9.3 Experimental Evidence for σ = 0.17

As an example, Wu et. al. (1991) studied primary breakup of round turbulent and non-turbulent jets of water, glycerol-water solutions, and n-Heptane in still air. They found Type I root normal size distributions with a lower bound of $\overline{R}_M \approx 1.1$, an upper bound of $\overline{R}_M \approx 1.5$, and an average of $\overline{R}_M \approx 1.2$. Three of the eighteen tests, those with relatively low jet speeds, approximately obtained the lower bound of $\overline{R}_M \approx 1.1$ or, equivalently, $\sigma \approx 0.17$ and $a = 1$.

As another example, Figure 10 compares Type I and II root normal distributions against experimental data obtained by Li and Tankin (1987) and Tischkoff (1979). The Type I and II distributions agree well except for the smallest droplets. Where the two distributions disagree, the experimental results slightly favor the Type II distribution.

9.4 Experimental Evidence for σ = 0.20

As an example, Empie et. al. (1993, 1995, 1997) conducted over 140 different experiments involving black liquor sprayed through vibrating and stationary splashplate, V-jet, and swirl cone nozzles. They found Type I root normal size distributions with a lower bound of $\sigma = 0.15$, an upper bound of $\sigma = 0.28$, and an arithmetic average of $\sigma = 0.20$. The tables and figures in Empie et. al. (1993) indicate that at least 16 of the experiments obtained $\sigma = 0.20$ almost exactly.

As another example, Figure 11 compares Type I and II root normal distributions against experimental data obtained by Turner and Moulton (1953). The Type I and II distributions agree well except for the smallest droplets. Where the two distributions disagree, the experimental results mostly favor the Type II distribution.

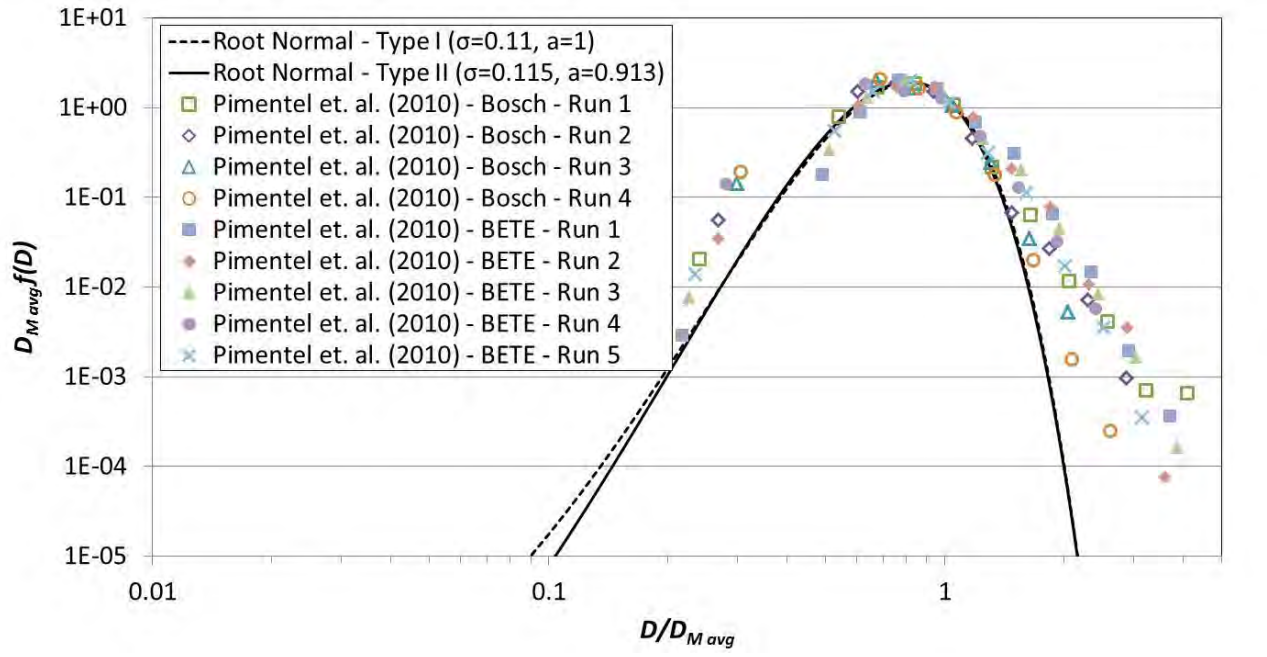

(a.) Log-log plane

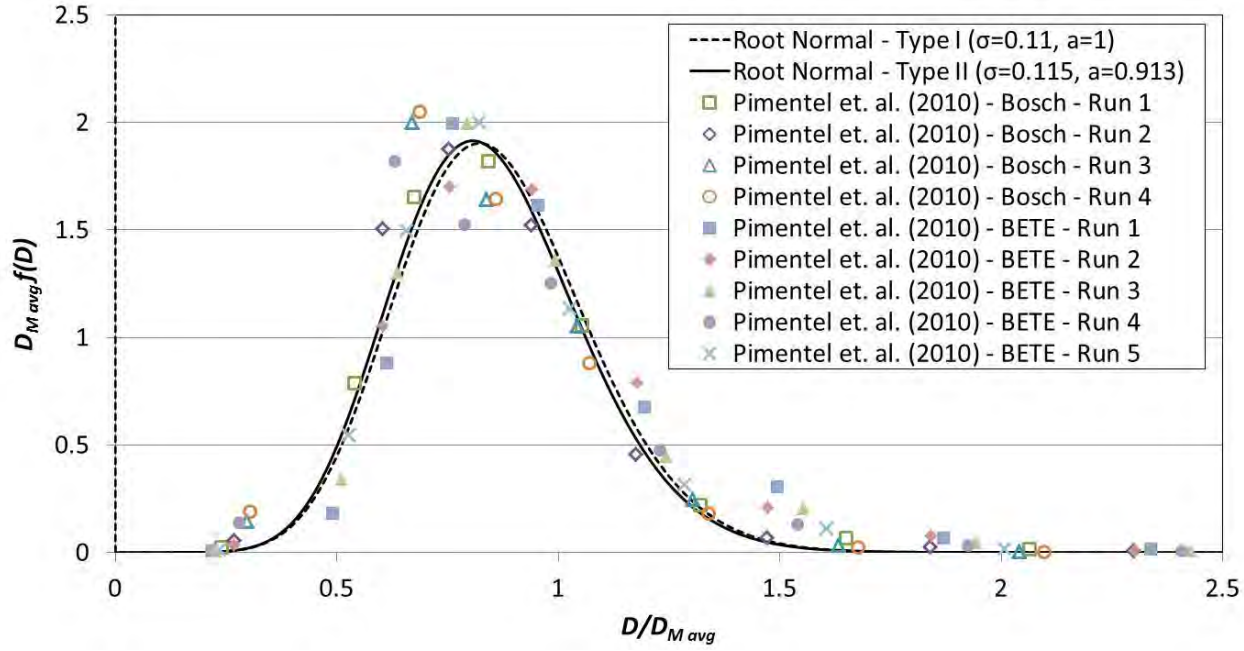

(b.) Linear-line plane

Figure 9. Type I vs. Type II root normal distributions compared to experimental results obtained by Pimentel et. al. (2010) using a common rail Bosch system and a BETE XA-PR200 nozzle.

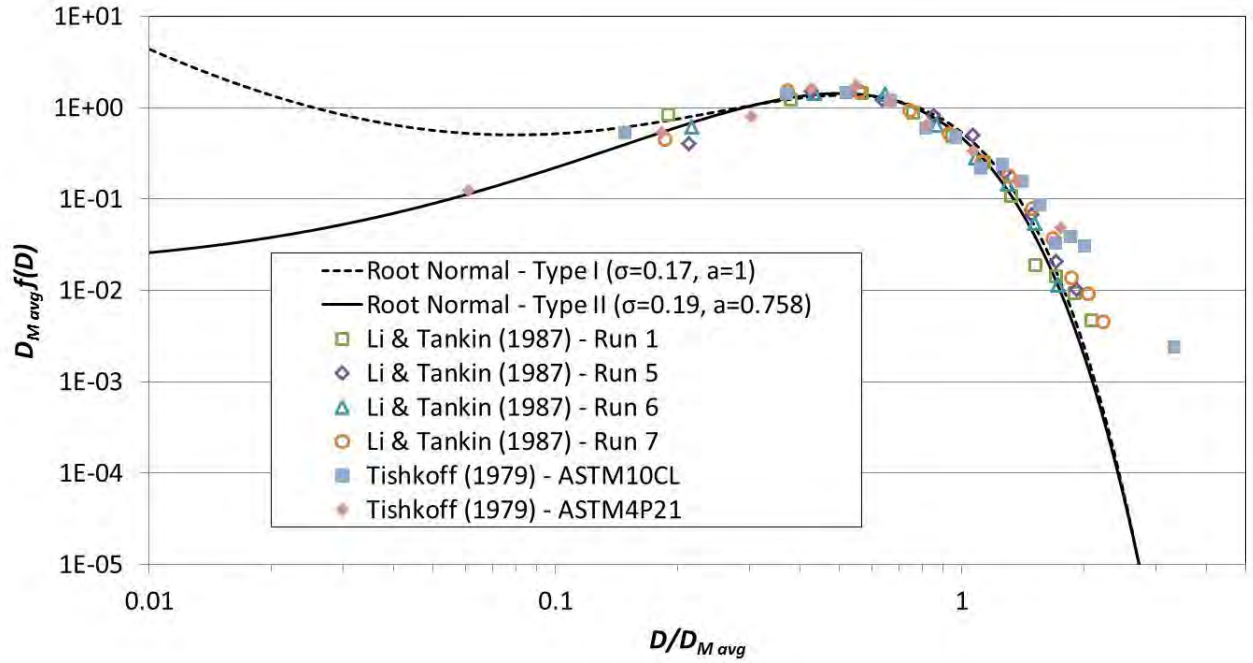

(a.) Log-log plane

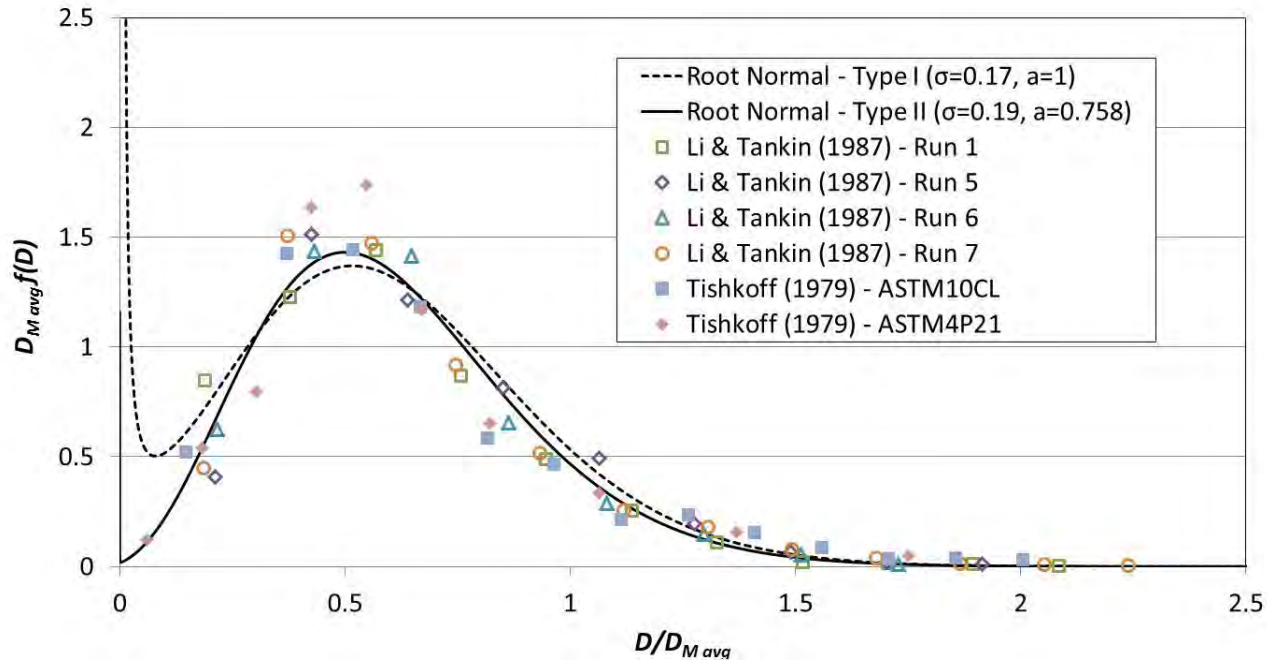

(b.) Linear-linear plane

Figure 10. Type I vs. Type II root normal distributions compared to experimental results obtained by Li and Tankin (1987) and Tischkoff (1979). Both sets of experimental results are as reported by Pimentel et. al. (2010).

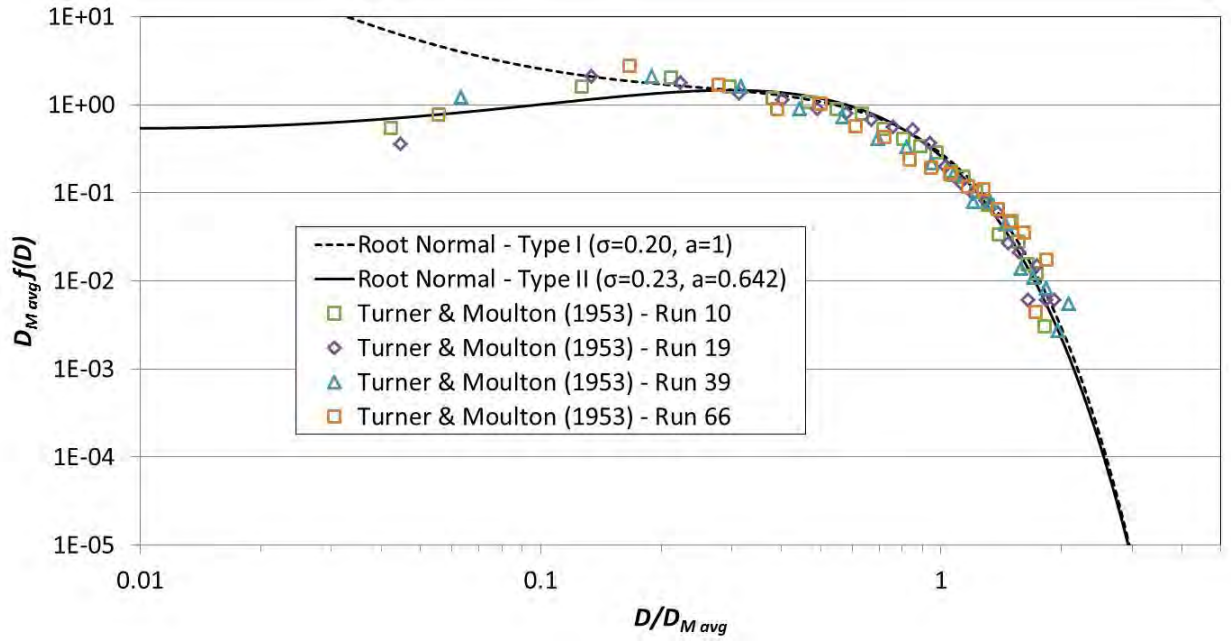

(a.) Log-log plane

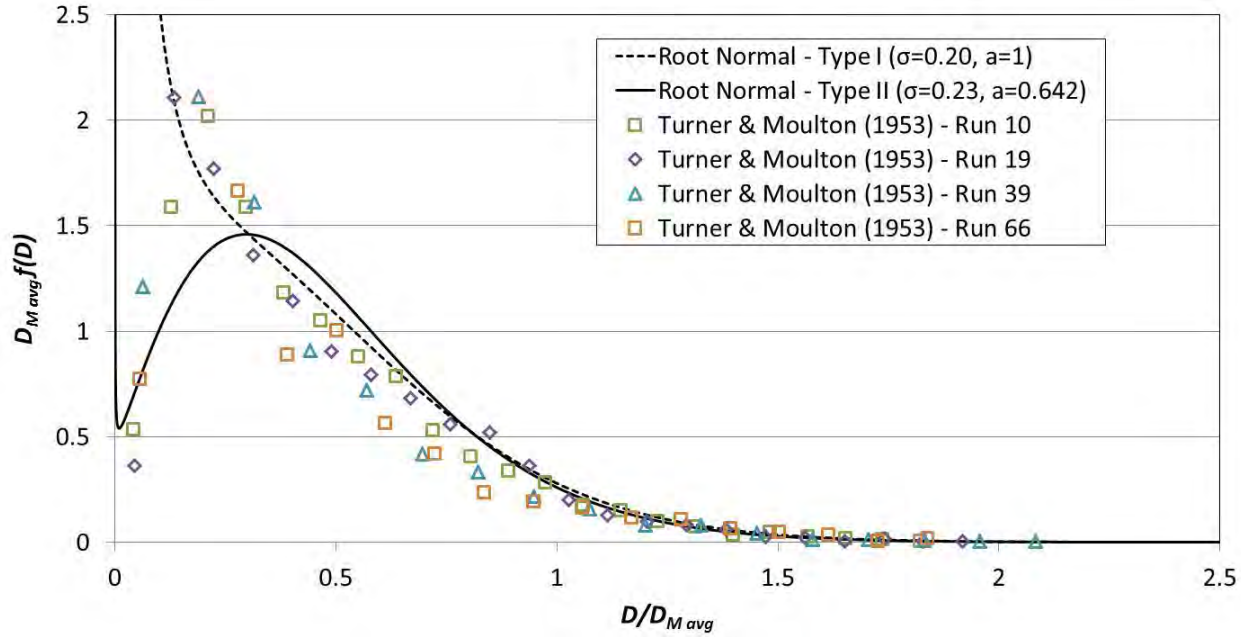

(b.) Linear-linear plane

Figure 11. Type I vs. Type II root normal distributions compared to experimental results obtained by Turner and Moulton (1953). The experimental results are as reported by Pimentel et. al. (2010).

9.5 Experimental Evidence for σ = 0.238

As a well-known example, Simmons (1977) examined "over 2,000 separate tests on about 100 different nozzle designs." According to Spielbauer et. al. (1989), the entire set of tests yielded Type I root normal sized distributions with an average σ of about "0.24, with a maximum 17% greater, and a minimum 20% smaller." Assuming $a = 1$, this roughly corresponds to a lower bound of $\overline{R}_M \approx 1.1$, an upper bound of $\overline{R}_M \approx 1.5$, and an average of $\overline{R}_M \approx 1.2$. For a subset of 200 tests "selected almost at random," Simmons (1977) reported a much narrower range of $\overline{R}_M \approx 1.20 \pm 5\%$. Simmons (1977) notes that $\overline{R}_M = 1.20$ corresponds to $\sigma = 0.238$ and $a = 1$.

As another example, Ruff et. al. (1992) studied primary and secondary breakup of laminar and turbulent round water jets in still air. They found Type I root normal size distributions with a lower bound of $\overline{R}_M \approx 1.1$, an upper bound of $\overline{R}_M \approx 1.5$, and an average of $\overline{R}_M \approx 1.2$. For both laminar and turbulent flows, they found $\overline{R}_M \approx 1.2$ at the jet surface. For laminar flows, they found $\overline{R}_M$ increased moving away from the jet surface, e.g., 1.10, 1.14, 1.22, 1.24. For turbulent flows, they found $\overline{R}_M$ decreased moving away from the jet surface, e.g., 1.27, 1.22, 1.18, 1.19.

As a third example, Hsiang and Faeth (1992, 1993) and Chou et. al. (1997) studied stripping-type breakup of liquid droplets moving through still air. In their schematic, aerodynamic forces cause a boundary layer to form on the surface of a droplet. Once the boundary layer becomes thick enough, it gradually sheds children droplets, whose mass mean diameters grow with the square root of time. Hsiang and Faeth (1992, 1993) represented all children from a given parent by a single size distribution, while Chou et. al. (1997) represented the children from a given parent by either three or four different size distributions. All told, Hsiang and Faeth (1992, 1993) and Chou et. al. (1997) reported stripping breakup results for fifteen different for combinations of liquid types and initial relative droplet velocities. Overall, they found Type I root normal size distributions with a lower bound of $\overline{R}_M \approx 1.1$, an upper bound of $\overline{R}_M \approx 1.5$, and an average of $\overline{R}_M \approx 1.2$. The test results were densely scattered between the upper and lower bounds without any obvious clustering around the boundaries or the average.

As a final example, Figure 12 compares Type I and II root normal distributions against experimental data obtained by Houghton (1941) and Tate and Olson (1979). The Type I and II distributions agree well except for the smallest droplets. Where the two distributions disagree, the experimental results clearly favor the Type II distribution. In the one result from Houghton (1941), the largest droplets appear to approximately obey a power law rather than a root normal size distribution.

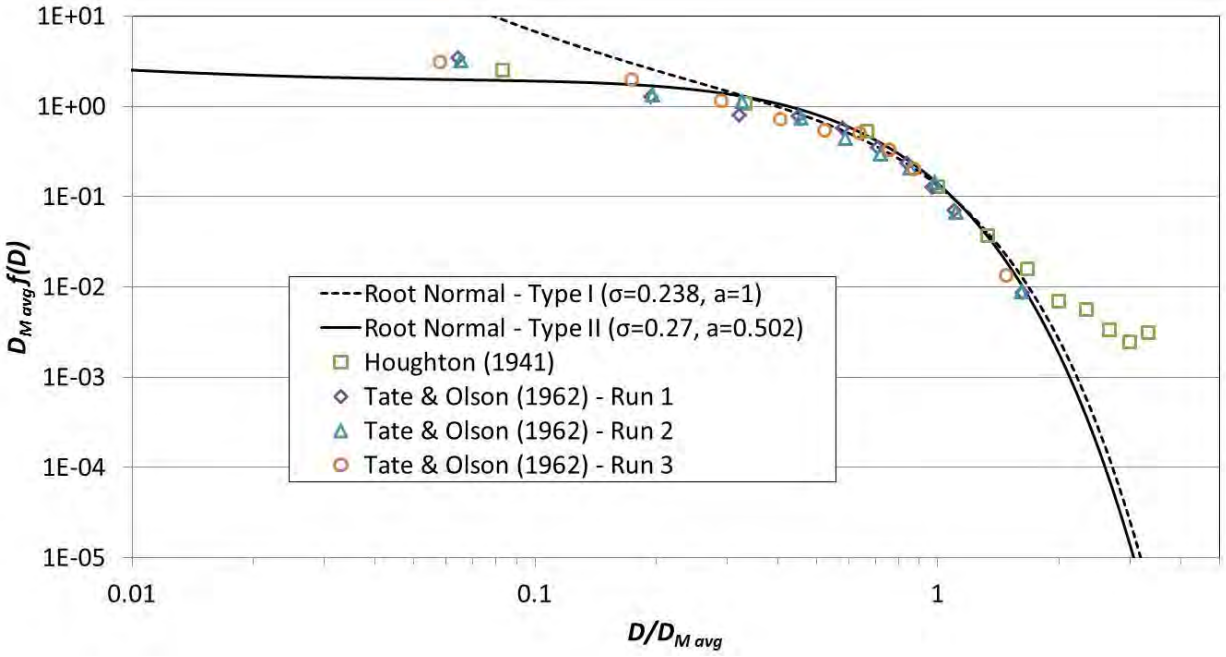

(a.) Log-log plane

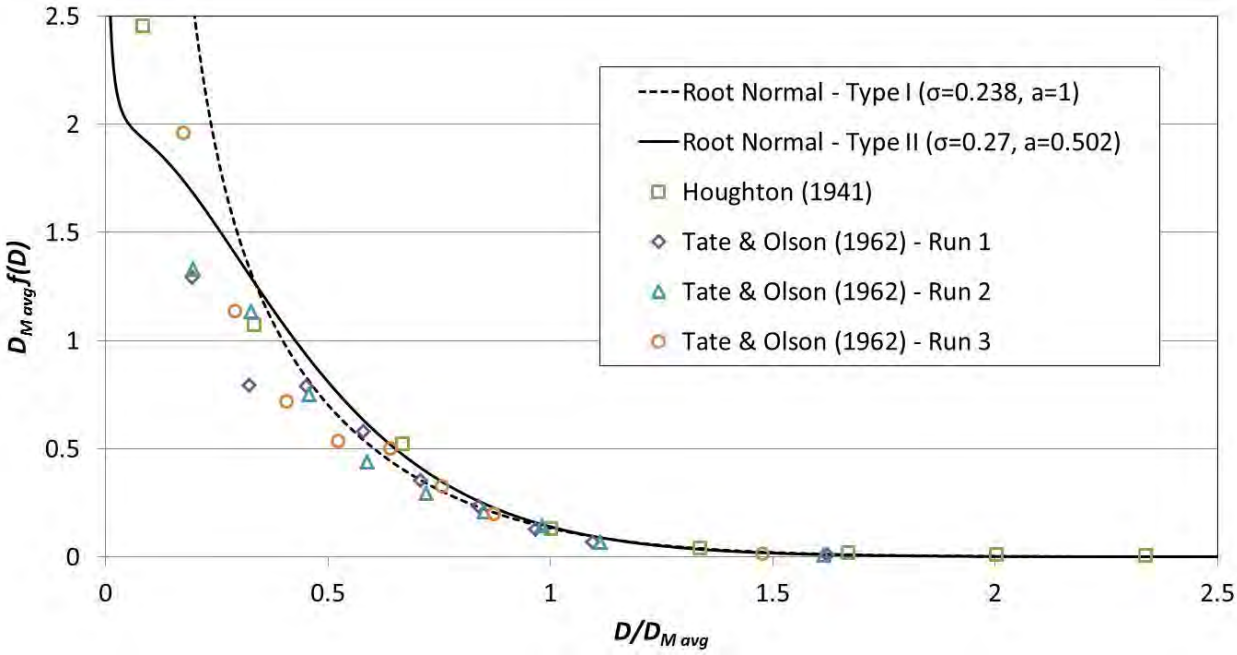

(a.) Linear-linear plane

Figure 12. Type I vs. Type II root normal distributions compared to experimental results obtained by Houghton (1941) and Tate and Olson (1962). The experimental results are as reported by Pimentel et. al. (2010).

As noted earlier, past researchers generally fitted experimental results in the probability-square-root plane, i.e., in a plane in which $1-F_M(D)$ is linear. To check the consistency between our fitting procedure and the traditional approach, Figure 13 coverts Figure 12 to a probability-square-root plane. The chosen root normal parameters appear to provide an equally good fit in either case. Notice that Φ is the cumulative distribution function of the standard normal distribution and Φ^{-1} is its inverse.

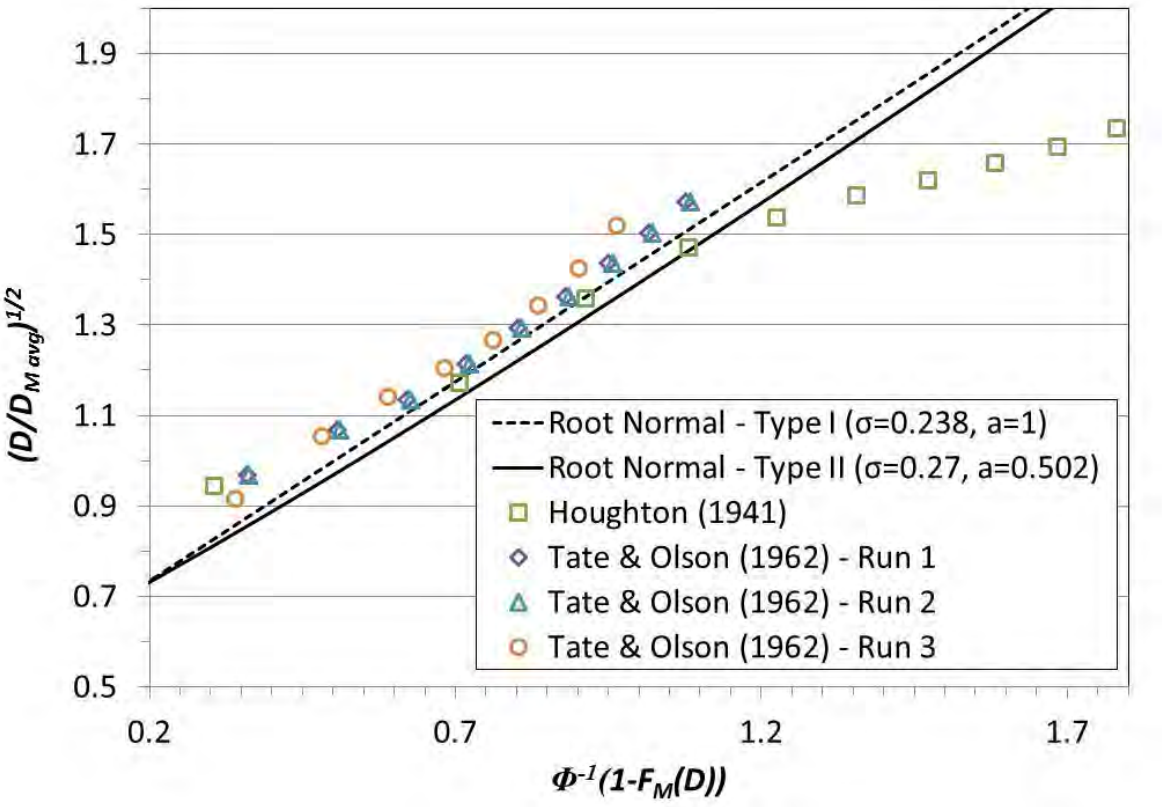

Figure 13. Another view of Type I vs. Type II root normal distributions compared to experimental results obtained by Houghton (1941) and Tate and Olson (1962). The experimental results are as reported by Pimentel et. al. (2010).

9.6 Experimental Evidence for σ = 0.286

As one example, Spielbauer et. al. (1989) sprayed black liquor through splashplate nozzles under varying conditions. They found 35 different root normal size distributions with a minimum value of $\sigma = 0.230$, a maximum value of $\sigma = 0.330$, and an arithmetic average value of $\sigma = 0.286$. Over 20% of the tests obtained the average value of $\sigma = 0.286$ almost exactly. For additional examples along these same lines, see Adams et. al. (1990) and Loebker & Empie (2001). None of the data in Pimentel et. al. (2010) is well-fitted by a Type I distribution with $\sigma = 0.286$; thus the plots seen in earlier cases are omitted here.

10. Conclusions

As summarized in Table 7, a small number of root normal size distributions, on the order of a half-dozen, may provide reasonably good fits to a wide variety of test data. No pretense is made that these are always the best possible fits. In particular, in many cases, root normal size distributions provide obviously poor fits to the largest droplets.

Table 7. Recommended Type IIA and Type IIB substitutes for the Type I distributions listed in Table 5.

	Original		**Recommended**			
	Type IA (*)		**Type IIA (*)**		**Type IIB (**)**	
	σ	a	σ	a	σ	a
1	0.081	1	0.083	0.9549	0.086	0.9963
2	0.11	1	0.115	0.9130	0.125	0.9922
3	0.17	1	0.19	0.7584	0.24	0.9708
4	0.20	1	0.23	0.6422	0.34	0.9389
5	0.238	1	0.27	0.5019	0.47	0.8650
6	0.286	1	0.33	0.2452	0.72	0.5738

(*) Normalized by the MMD (**) Normalized by the CMD.

Unlike other size distributions, the parameters in root normal size distributions depend on which average size, such as the MMD or CMD, is used for normalization. As seen in Table 7, the difference is small only when σ is small.

While not always an exact match to the traditional Type I distributions, the Type II and IIB distributions given in Table 7 avoid severe singularities found in the Type I distributions, and ensure true self-similarity. Furthermore, the preponderance of the experimental evidence reviewed here favors Type II over Type I root normal size distributions.

As seen in Section 9, most previous work on root normal size distributions relies on heavily-averaged test data. First, the results for each test are usually averaged over time and/or space. In those rare cases where test results are given for specific points in time and/or space, the results often deviate substantially from the average, e.g., Ruff et. al. (1992), Chou et. al. (1997). Next, the results are usually averaged across multiple test, sometimes dozens or even hundreds of different tests with different outcomes. When results are given for one specific test, the results often deviate substantially from the average.

As a typical conclusion based on such averages-of-averages, Spielbauer et. al. (1989) says that the "size distribution doesn't change, or changes very little, as a function of nozzle geometry, flow conditions, and fluid parameters … What is most surprising … is the similarity of the droplet size distribution from the splashplate and swirl cone nozzles." While ±15% or ±20% variations in root normal parameters such as σ may seem small, the results given here show that they can be highly significant, although this obviously depends on the application.

By focusing on individual tests rather than ensemble averages of different tests, this treatment has avoided one kind of averaging. However, it is hard to avoid the other kind of averaging –

individual test results may still depend on averages in time and/or space. Accurate pre-test prediction is difficult to the extent that test results depend on unknowns such as exactly when or where measurements will be taken.

The results presented here indicate that the well-known Simmons universal root normal size distribution may not always be especially common. In particular, for the data compiled by Pimentel et. al. (2010), Simmons universal root normal provides the best fit just about 10% of the time; see Table 6. Obviously, this observation only applies to one particular collection of test data. Different collections of test data have, in the past, yielded very different conclusions. Future work will hopefully provide additional insight into the correctness, completeness, and frequency of occurrence of the root normal parameters surveyed here.

Acknowledgments

This work was supported by the Nuclear Effects Office of the Defense Threat Reduction Agency (DTRA). The author wishes to thank Dr. John Cockayne of Leidos Inc. for his contributions.

References

C. Aalburg, B. Van Leer, G.M. Faeth, and K.A. Sallam, Properties of Nonturbulent Round Liquid Jets in Uniform Gaseous Crossflows," *Atomization and Sprays*, 15(3), 271-294, 2005

T. N. Adams, H. L. Empie, N. Obuskovic, and T. M. Spielbauer, *Kraft Black Liquor Delivery Systems Report No. 1*, Institute of Paper Science and Technology Technical Report, February 1990

N. Ashgriz, Editor, *Handbook of Atomization and Sprays: Theory and Applications*, Springer, 2011

E. Babinsky and P. E. Sojka, Modeling Drop Size Distributions, *Progress in Energy and Combustion Science*, 28, 303-329, 2002

L. P. Bayvel and Z. Orzechowski, *Liquid Atomization*, Taylor and Francis, 1993

J. C. Bhatia, J. Domnick, F. Durst, and C. Tropea, Phase-Doppler Anemometry and the Log-Hyperbolic Distribution Applied to Liquid Sprays, *Particle and Particle Systems Characterization*, 5(4), l53-164, 1988

C. E. Brennan, *Fundamentals of Multiphase Flows*, Cambridge University Press, 2005

W. K. Brown, A Theory of Sequential Fragmentation and Its Astronomical Applications, *Journal of Astrophysics and Astronomy*, 10(1), 89-112, 1989

W. K. Brown and K. H. Wohletz, Derivation of the Weibull Distribution Based on Physical Principles and Its Connection to the Rosin–Rammler and Lognormal Distributions, *Journal of Applied Physics*, 78(4), 2758-2763, 1995

W.-H. Chou, L.-P. Hsiang, and G. M. Faeth, Temporal Properties of Drop Breakup in the Shear Breakup Regime, *International Journal of Multiphase Flow*, 23, 651-669, 1997

W.-H. Chou and G. M. Faeth, Temporal Properties of Secondary Drop Breakup in the Bag Breakup Regime, *International Journal of Multiphase Flow*, 24, 889-912, 1998

A. Clauset, C. R. Shalizi, and M. E. J. Newman, Power-Law Distributions in Empirical Data, *SIAM Review*, 51(4), 661–703, 2009

C. T. Crowe, Editor, *Multiphase Flow Handbook*, CRC Press, 2006

Z. Dai, W.-H. Chou, and G. M. Faeth, Drop Formation Due to Turbulent Primary Breakup at the Free Surface of Plane Liquid Wall Jets, *Physics of Fluids*, 10, 1147-1157, 1998

C. Dumouchel, The Maximum Entropy Formalism and the Prediction of Liquid Spray Drop-Size Distribution, *Entropy*, 11, 713-747, 2009

C. Dumouchel, J.-B. Blaisot, and V.D. Ngo, On the Adequacy Between the Laser Diffraction Diameter Distribution and the 3-parameter Generalized-Gamma function, *Chemical Engineering Science*, 79, 103, 2012

H. J. Empie, S. J. Lien, R. S. Rumsey, and D. G. Sachs, *Kraft Black Liquor Delivery Systems Report No.4*, Institute of Paper Science and Technology Technical Report, January 1993

H. J. Empie, S. J. Lien, W. Yang, and T. N. Adams, Spraying Characteristics of Commercial Black Liquor Nozzles, *TAPPI Journal*, 78(1), 121-128, 1995

H. J. Empie, S. J. Lien, and W. Yang, Drop Size Modification in Black Liquor Sprays From Commercial Nozzles Using Pulsed Flow, *Atomization and Sprays*, 7, 457-466, 1997

S. K. Friedlander and C. Wang, The Self-Preserving Particle Size Distribution for Coagulation by Brownian Motion, *Journal of Colloid and Interface Science*, 22, 126–32, 1966

H. G. Houghton in J. H. Perry, Editor, *Perry's Chemical Engineers' Handbook, 2nd ed.*, McGraw-Hill, 1941

L.-P. Hsiang and G. M. Faeth, Near-Limit Drop Deformation and Secondary Breakup, *International Journal of Multiphase Flow*, 18, 635-652, 1992

L.-P. Hsiang and G. M. Faeth, Drop Deformation and Breakup Due to Shock Wave and Steady Disturbances, *International Journal of Multiphase Flow*, 21, 545-560, 1993

D. D. Joseph, J. Belanger, and G. S. Beavers, Breakup of a Liquid Drop Suddenly Exposed to a High-Speed Airstream, *International Journal of Multiphase Flow*, 25, 1263-1303, 1999

D. D. Joseph, G. S. Beavers, and T. Funada, Rayleigh–Taylor Instability of Viscoelastic Drops at High Weber Numbers, *Journal of Fluid Mechanics*, 453, 109-132, 2002

K. Lee, C. Aalburg, F. J. Diez, G. M. Faeth, and K. A. Sallam, Primary Breakup of Turbulent Round Liquid Jets in Uniform Crossflows, *AIAA Journal*, 45(8), 2007

K. W. Lee, H. Chen, and J. A. Gieske, Log-Normally Preserving Size Distribution for Brownian Coagulation in the Free-Molecular Regime, *Aerosol Science and Technology*, 3, 53-62, 1984

K. E. J. Lehtinen and M. R. Zachariah, Self-Preserving Theory for the Volume Distribution of Particles Undergoing Brownian Coagulation, *Journal of Colloid and Interface Science*, 242, 314-318, 2001

Li, X. and Tankin, R. S., Droplet Size Distribution: A Derivation of a Nukiyama-Tanasawa Type Distribution Function, *Combustion Science and Technology*, 65–76, 1987

H. Liu, *Science and Engineering of Droplets: Fundamentals and Applications*, William Andrew Publishing, 2000

D. W. Loebker and H. J. Empie, Independently Controlled Drop Size in Black Liquor Sprays into the Kraft Recovery Boiler Using Effervescent Atomization, *Journal of Pulp and Paper Science*, 27(1), 18-25, 2001

B. Miller, K.A. Sallam, M. Bingabr, K.-C. Lin, and C. Carter, Breakup of Aerated Liquid Jets in Subsonic Crossflow," *Journal of Propulsion and Power*, 24(2), 253-258, 2008

R. Pimentel, R. Stowe, P. Harris, A. DeChamplain, and D. Kretschmer, Spray Characterization Based on the Pearson System of Frequency Curves, *Atomization and Sprays*, 20(5), 365-386, 2010

T. Paloposki and N. E. Fagerholm, *The Atomization of Heavy Fuel Oil with Swirl Pressure Jet Atomizer*, Helsinki University of Technology, Institute of Energy Engineering Research Report TKK-KO/ET-13, NTIS Accession Number DE87751107, 1986

T. Paloposki, Drop Size Distributions in Liquid Sprays, *Acta Polytechnica Scandinavica*, Mechanical Engineering Series 114, Helsinki, Finland, 1994

G. A. Ruff, P.-K. Wu, L. P. Bernal and G. M. Faeth, Continuous- and Dispersed-Phase Structure of Dense Nonevaporating Pressure-Atomized Sprays, *Journal of Propulsion and Sprays*, 8(2), 1992

K. A. Sallam, Z. Dai, and G. M. Faeth, Drop Formation at the Surface of Plane Turbulent Liquid Jets in Still Gases, *International Journal of Multiphase Flow*, 25, 1161-1180, 1999

K.A. Sallam, C. Aalburg, G.M. Faeth, K.-C. Lin, C.D. Carter, and T.A. Jackson, Primary Breakup of Round Aerated-Liquid Jets in Supersonic Crossflows, *Atomization and Sprays*, 16(6), 657-672, 2006

H. C. Simmons, The Correlation of Drop-Size Distributions in Fuel Nozzle Spray, Parts I and II, *Journal of Engineering for Power*, 99, 309-319, 1977

P. T. Spicer and S. E. Pratsinis, Coagulation and Fragmentation: Universal Steady-State Particle-Size Distribution, *AIChE Journal*, 42, 1612-1620, 1996

T. M. Spielbauer, T. N. Adams, J. E. Monacelli, and R. T. Bailey, Droplet Size Distribution of Black Liquor Sprays, *1989 International Chemical Recovery Conference*, Ottawa, Canada, TAPPI/CPPA, 1989

R. W. Tate and W. R. Marshall Jr., Atomization by Centrifugal Pressure Nozzles, *Chemical Engineering Progress*, 49, 169–174, 1953

R. W. Tate and E. O. Olson, Spray Droplet Size of Pressure-Atomizing Burner Nozzles, *ASHRAE Journal*, 4(3), 39-43, 1962

J. M. Tishkoff, *GMR Laser-video Imaging System Results for the ASTM 'Round-Robin' Nozzle Test*, General Motors Research Publication GMR-3098, 1979

G. M. Turner and R. W. Moulton, Drop Size Distributions from Spray Nozzles, *Chemical Engineering Progress*, 49(4), 185-190, 1953

T. G. Theofanous, Aerobreakup of Newtonian and Viscoelastic Liquids, *Annual Review Fluid Mechanics*, 43, 661–690, 2011

P.-K. Wu, G. A. Ruff, and G. M. Faeth, Primary Breakup in Liquid-Gas Mixing Layers, *Atomization and Sprays*, 1, 421-440, 1991

P.-K. Wu, L.-K. Tseng, and G. M. Faeth, Primary Breakup in Gas/Liquid Mixing Layers for Turbulent Liquids, *Atomization and Sprays*, 295-317, 1992

P.-K. Wu and G. M. Faeth, Aerodynamic Effects on Primary Breakup of Turbulent Liquids, *Atomization and Sprays*, 3, 265-289, 1993

P.-K. Wu, R. F. Miranda, and G. M. Faeth, Effects of Initial Flow Conditions on Primary Breakup of Nonturbulent and Turbulent Round Liquid Jets, *Atomization and Sprays*, 5, 175-196, 1995

DEPARTMENT OF DEFENSE

DEFENSE THREAT REDUCTION
AGENCY
8725 JOHN J. KINGMAN ROAD
STOP 6201
FORT BELVOIR, VA 22060
ATTN: CAPT PAUL
CLEMENT

DEFENSE TECHNICAL
INFORMATION CENTER
8725 JOHN J. KINGMAN ROAD,
SUITE 0944
FT. BELVOIR, VA 22060-6201
ATTN: DTIC/OCA

DEPARTMENT OF DEFENSE
CONTRACTORS

QUANTERION SOLUTIONS, INC.
1680 TEXAS STREET, SE
KIRTLAND AFB, NM 87117-5669
ATTN: DTRIAC